

Bethe M -layer construction for the percolation problem

Maria Chiara Angelini^{1,2}, Saverio Palazzi^{1*}, Tommaso Rizzo^{1,3} and Marco Tarzia^{4,5}

1 Dipartimento di Fisica, Sapienza Università di Roma, Piazzale A. Moro 2, I-00185, Rome, Italy

2 INFN-Sezione di Roma 1, Piazzale A. Moro 2, 00185, Rome, Italy

3 ISC-CNR, UOS Rome, Sapienza Università di Roma, Piazzale A. Moro 2, I-00185, Rome, Italy

4 LPTMC, CNRS-UMR 7600, Sorbonne Université, 4 Pl. Jussieu, F-75005 Paris, France

5 Institut Universitaire de France, 1 rue Descartes, 75231 Paris Cedex 05, France

* saverio.palazzi@uniroma1.it

Abstract

One way to perform field theory computations for the bond percolation problem is through the Kasteleyn and Fortuin mapping to the $n + 1$ states Potts model in the limit of $n \rightarrow 0$. In this paper, we show that it is possible to recover the ϵ -expansion for critical exponents in finite dimension directly using the M -layer expansion, without the need to perform any analytical continuation. Moreover, we also show explicitly that the critical exponents for site and bond percolation are the same. This computation provides a reference for applications of the M -layer method to systems where the underlying field theory is unknown or disputed.

Copyright attribution to authors.

This work is a submission to SciPost Physics.

License information to appear upon publication.

Publication information to appear upon publication.

Received Date

Accepted Date

Published Date

1

2 Contents

3	1 Introduction	2
4	2 Models and main results	3
5	3 Percolation on the Bethe Lattice	5
6	4 The M-layer expansion	8
7	5 M-layer for percolation in D dimensions	10
8	6 Computation of critical exponents	17
9	7 Conclusion	22
10	A Identification of the constants in the M-layer expansion	22
11	B Connection with field theoretical expressions	24

12	C Other diagrams	25
13	D Four-point correlation function	27
14	References	31

17 1 Introduction

18 The percolation problem provides one of the simplest examples of a second-order phase tran-
 19 sition, in both the versions of site or bond percolation. Despite the simplicity of the model, it is
 20 at the basis of different problems in many different fields, from condensed matter to telecom-
 21 munication engineering, from graph theory to epidemic spreading [1, 2]. In the standard site
 22 (bond) percolation problem, each site (bond) is present independently of the neighbors with
 23 probability p . Above a certain threshold p_c , a giant cluster of nearest-neighbor sites is present
 24 in the thermodynamic limit while below this threshold neighboring sites are grouped into many
 25 small clusters of non-extensive size. The value p_c corresponds to the transition point and one
 26 can associate standard critical exponents that describe how critical observables behave near
 27 p_c . Despite the deep similarities with respect to critical behavior, the main difference between
 28 percolation and other phase transition models is the absence of an associated Hamiltonian and
 29 a corresponding partition function.

30 The renormalization group (RG) is the main tool to study second order phase transitions.
 31 It can be applied in two ways: the first one is by performing explicitly an RG transformation
 32 on a given two- or three-dimensional lattice while the second relies on field theory. The first
 33 method typically requires uncontrolled approximations (needed to close the RG equations and
 34 find a fixed point) while the second is more powerful as it allows one to systematically obtain
 35 the critical exponents in dimension D in powers of $\epsilon = D_U - D$ where D_U is the upper critical
 36 dimension. The first method can be applied to percolation as it is [3, 4] but one could think
 37 that the lack of a Hamiltonian would make the application of the second impossible. However,
 38 in a seminal paper, Kasteleyn and Fortuin showed that the bond percolation problem is exactly
 39 related to the $n \rightarrow 0$ limit of an n -component ($n + 1$ states) Potts model [5]. It was then
 40 recognized [6] that this mapping allows the application of field-theoretical techniques and
 41 today the exponents are known up to the 5th order in an ϵ -expansion around the upper critical
 42 dimension [7–11].

43 In this paper, we reproduce the same expansion up to one-loop order by means of the M -
 44 layer construction. This construction has been introduced in Ref. [12], and then applied to a
 45 variety of models [13–18]. The useful property of the M -layer construction is that one can
 46 also study the critical behavior, in finite dimensions, of problems which are not defined by a
 47 Hamiltonian, such as the percolation. One has to introduce $M - 1$ independent lattices, in
 48 addition to the original one; the M layers will then be coupled together through a random
 49 rewiring of the bonds. The $M \rightarrow \infty$ limit gives the Bethe lattice solution [19] of the model,
 50 while if $M = 1$ one obtains the original model. An expansion in $1/M$ can be properly set
 51 up, that is in practice an expansion in the number of the topological loops considered. The
 52 M -layer construction can be applied to any model that can be defined on a locally tree-like
 53 graph, including percolation. This is interesting, because, with this approach, there is no need
 54 to invoke the $n \rightarrow 0$ analytic continuation discovered by Kasteleyn and Fortuin. Furthermore,
 55 with this method, we can also analytically verify that the critical exponents of site percolation
 56 are equal to those of bond percolation.

57 The additional value of this paper is methodological: we show for the first time that from
 58 the $1/M$ expansion on the M -layer lattice one can obtain the ϵ -expansion, through the suitable
 59 introduction of a dimensionless beta function in analogy with what is usually done in standard
 60 field theory [20, 21]. This is a fundamental step that will help in applying in the future the
 61 same techniques to more complicated systems, for which a finite-dimensional solution is still
 62 not known, such as the Edward-Anderson spin-glass model [17] or Anderson localization [18].

63 The paper is organized as follows: In Section 2 we present the model and the main results,
 64 in particular we sketch the derivation of the ϵ -expansion for the critical exponents from the
 65 $1/M$ expansion of two- and three-point correlation functions. In Section 3 we introduce the
 66 problem on the Bethe lattice with a novel derivation of the cluster distribution function. In
 67 Section 4 we recall the general properties of the $1/M$ expansion and the operative rules to
 68 compute it. In Section 5 we present the computation of the observables in the M -layer frame-
 69 work for both site and bond percolation. In Section 6 we apply one of the standard methods
 70 to compute critical exponents in ϵ -expansion. Finally, in Section 7, we give our conclusions.

71 2 Models and main results

72 In this Section we list the results of the application of the M -layer construction to both the bond
 73 and site percolation problems on a hyper-cubic lattice in D dimensions. We briefly describe
 74 the steps needed to reach the final results which will be summarized next.

75 In the standard site (respectively bond) percolation problem, each site (respectively bond)
 76 is present, or “active”, independently of the neighbors with probability p . In the site percola-
 77 tion problem one then defines a cluster as a subset of nearest-neighbor active sites, while in
 78 bond percolation a cluster is defined as a subset of sites connected by nearest-neighbor active
 79 bonds. At p_c a giant cluster appears, that contains a finite fraction of all the sites N . Our
 80 analysis will mainly apply to the non-percolating phase $p < p_c$ and from now on we refer to
 81 this case. The critical behavior in the non-percolating phase is characterized by considering
 82 the average number $n(s, p)$ of clusters of size s in a system of size N . This distribution is cut
 83 off at a typical size s^* that diverges at the critical point. We also consider the q -point function
 84 $C_q(\mathbf{x}_1, \dots, \mathbf{x}_q)$ that gives the probability that the sites at $\mathbf{x}_1, \dots, \mathbf{x}_q$ belong to the same clus-
 85 ter. According to scaling arguments [1, 22], we expect that the two-point function obeys the
 86 following scaling form for large $|\mathbf{x}_1 - \mathbf{x}_2|$ and for p close to p_c :

$$C_2(\mathbf{x}_1, \mathbf{x}_2) = \frac{1}{|\mathbf{x}_1 - \mathbf{x}_2|^{D-2+\eta}} f_{C_2} \left(\frac{|\mathbf{x}_1 - \mathbf{x}_2|}{\xi} \right), \quad (1)$$

87 where f_{C_2} is a proper scaling function, η is the anomalous dimension and ξ is the correlation
 88 length that diverges at the critical point as:

$$\xi \sim \frac{1}{|p - p_c|^\nu}. \quad (2)$$

89 The typical size s^* scales with the correlation length as

$$s^* \sim \xi^{D_f}, \quad (3)$$

90 where D_f stands for the fractal dimension of the clusters. The distribution of the cluster sizes
 91 also obeys a scaling law [1, 22]:

$$n(s, p) = s^{-\tau} f_n(|p - p_c| s^\sigma), \quad (4)$$

92 where $f_n(\mathbf{x})$ is another scaling function. We also consider the space integrals of the $C_q(\mathbf{x}_1, \dots, \mathbf{x}_q)$,
 93 called susceptibilities,

$$\chi_q \equiv \sum_{\mathbf{x}_2, \dots, \mathbf{x}_q} C_q(\mathbf{x}_1, \dots, \mathbf{x}_q) \quad (5)$$

94 that are independent of \mathbf{x}_1 in a homogeneous system (they only depend on the differences
 95 between the points). They are related to the moments of the $n(\mathbf{s}, \mathbf{p})$ through:

$$\chi_q = \sum_{s=0}^{\infty} s^q n(\mathbf{s}, \mathbf{p}). \quad (6)$$

96 The scalings of the typical size s^* and the correlation length ξ give

$$\sigma = \frac{1}{\nu D_f}, \quad (7)$$

97 while, given the relation

$$\tau = 1 + \frac{D}{D_f}, \quad (8)$$

98 comparing Eqs. (5) and (6) and using the scaling of $n(\mathbf{s}, \mathbf{p})$ one can easily find that the
 99 susceptibilities diverge as

$$\chi_q \sim \xi^{-D+D_f q}, \quad (9)$$

100 from which it follows that the following quantity goes to a constant at the critical point:

$$\lambda \propto \xi^{-D} \frac{\chi_3^2}{\chi_2^3}. \quad (10)$$

101 On the M -layer lattice χ_2 and χ_3 are given by the Bethe lattice solution in the limit $M \rightarrow \infty$
 102 and we computed the first $1/M$ correction, for both site and bond percolation. Once the two-
 103 point observable is computed, with the M -layer construction, the upper critical dimension, D_U ,
 104 can be deduced from the Ginzburg criterion and for the percolation problem it turns out to be
 105 $D_U = 6$. At this point of the computation a standard procedure to compute critical exponents
 106 is applied [20]. In particular we write λ as:

$$\lambda = u - \frac{7}{4} \frac{u^2}{(4\pi)^{\frac{D}{2}}} \Gamma\left(3 - \frac{D}{2}\right) + \mathcal{O}(u^3), \quad (11)$$

107 where the constant u is defined as $u \equiv g m^{D-6}$, where $m \equiv \xi^{-1}$ and g is a $\mathcal{O}(1/M)$ constant
 108 that depends on the microscopic details of the model including whether we consider bond or
 109 site percolation. Note that the dimensionless constant u diverges at the critical point for $D < 6$
 110 because m vanishes, while λ remains finite at the critical point according to Eq. (9). Notice
 111 that, in order to understand this last statement from Eq. (11), one should consider the relation
 112 between λ and u to all orders in u , but in this perturbative framework we only compute the
 113 first correction, to $\mathcal{O}(u^2)$. We expect that:

$$\lambda \approx \lambda_c + c_1 \xi^\omega = \lambda_c + c_1 m^{-\omega}, \quad \text{for } \xi \rightarrow \infty, m \rightarrow 0 \quad (12)$$

114 where c_1 is a model-dependent constant, while ω is a universal exponent that controls the
 115 corrections to scaling [20]. Now, following a standard field-theoretical procedure (see Ref.
 116 [20], Chap. 8), we define the function $b(\lambda)$, using the above relationships:

$$b(\lambda) \equiv m^2 \frac{\partial}{\partial m^2} \lambda \approx -\frac{\omega}{2} c_1 m^{-\omega} \approx -\frac{\omega}{2} (\lambda - \lambda_c), \quad (13)$$

117 meaning that at the critical point

$$b(\lambda_c) = 0, \quad \omega = -2b'(\lambda_c). \quad (14)$$

118 From (11), we obtain an expression of $b(\lambda)$ to second order in λ from which the following
 119 scenario emerges: for $D \geq D_U = 6$ only the solution $\lambda = 0$ exists, meaning that λ tends to zero
 120 at the critical point with $\omega = 6 - D$, while for $\epsilon \equiv 6 - D > 0$ a new solution $\lambda_c \neq 0$ appears:

$$\lambda_c = \frac{2(4\pi)^3}{7} \epsilon + \mathcal{O}(\epsilon^2) \quad (15)$$

121 and λ tends to λ_c at the critical point, with $\omega = -\epsilon + \mathcal{O}(\epsilon^2)$. Here the universality is realized:
 122 the non-trivial fixed point λ_c doesn't depend anymore on the specific value of g and thus it
 123 doesn't depend on the microscopic details of the system (including if we are dealing with bond
 124 or site percolation). Moreover we confirm that, due to universality, the values of the critical
 125 exponents do not depend on the value of M .

126 Following similar standard computations (see Ref. [20], Chap. 8), from the value of λ_c
 127 and the scaling laws, we obtained the ϵ -expansion for the critical exponents:

$$\nu = \frac{1}{2} + \frac{5}{84} \epsilon + \mathcal{O}(\epsilon^2), \quad (16)$$

128

$$\eta = -\frac{1}{21} \epsilon + \mathcal{O}(\epsilon^2). \quad (17)$$

129 Comparing Eq. (9) with the scaling law $\chi_2 \sim \xi^{2-\eta}$ we obtain

$$D_f = \frac{D + 2 - \eta}{2}, \quad (18)$$

130 all the other critical exponents can be obtained from η and ν through the scaling laws given
 131 above.

132 We stress that the result is independent of the actual values of any non-universal constant,
 133 ensuring that the critical exponents are the same for bond and site percolation, as explained
 134 more extensively in Sec. 5. As it should, the results coincide with those obtained from the
 135 ϵ -expansion for the $(n + 1)$ -state Potts models in the limit $n \rightarrow 0$, which coincides with bond
 136 percolation according to the Fortuin-Kasteleyn mapping. In appendix D we have also computed
 137 the expansion of χ_4 in powers of $1/M$ checking that it diverges at the critical point with an
 138 exponent equal to that predicted by Eq. (9).

139 3 Percolation on the Bethe Lattice

140 In this Section we show how to derive equations for the critical behavior of $g(\mathbf{s}, \mathbf{p})$, defined
 141 as the probability that a randomly chosen site belongs to a cluster of size \mathbf{s} , including $\mathbf{s} = \mathbf{0}$
 142 meaning that the site is not active. We discuss the case of site percolation on a Bethe lattice
 143 and how to derive the exact critical exponents in this case. Given the definition of $n(\mathbf{s}, \mathbf{p})$, in
 144 Sec. 2, we have

$$g(\mathbf{0}, \mathbf{p}) = (1 - p); \quad g(\mathbf{s}, \mathbf{p}) = s n(\mathbf{s}, \mathbf{p}) \text{ for } \mathbf{s} > \mathbf{0}. \quad (19)$$

145 Here and in the following we call ‘‘Bethe lattice’’ a random regular graph with fixed connectivity
 146 c . Notice that $g(\mathbf{s}, \mathbf{p})$ as it should is normalized to 1 because the probability that a randomly
 147 chosen site belongs to a cluster is $\sum_{\mathbf{s}} s n(\mathbf{s}, \mathbf{p}) = p$. We also define the associated ‘‘cavity’’
 148 probability, $g_{cav}(\mathbf{s}, \mathbf{p})$, as the probability that a randomly chosen site, for which one of its c

149 edges is removed, belongs to a cluster of size s . This definition is useful since on a Bethe
 150 lattice two sites are connected by a unique sequence of adjacent edges, so that, removing one
 151 edge, the two sites will be completely independent and the resulting probability to belong to
 152 a cluster factorizes [23]. Thus, given that each site is active with probability p , we can write
 153 a self-consistent equation for $g_{cav}(s, p)$ on the Bethe lattice with fixed connectivity c :

$$g_{cav}(s, p) = (1-p) \delta_{s,0} + p \sum_{s_1=0}^{\infty} \cdots \sum_{s_{c-1}=0}^{\infty} g_{cav}(s_1, p) \cdots g_{cav}(s_{c-1}, p) \delta_{s,1+s_1+\cdots+s_{c-1}}, \quad (20)$$

154 where the first term comes from the case in which the given site is not present, and the resulting
 155 size of the cluster is $s = 0$, while the second is the probability that the site is present, p , times
 156 the product of the factorized probabilities that the $c-1$ neighboring sites (one edge is removed,
 157 see Fig. 1) belong to clusters of sizes s_1, s_2, \dots, s_{c-1} . In this second case the resulting size
 158 must be the sum of the sizes plus one, the given site. The probability $g(s, p)$ can then be
 159 expressed in terms of the cavity probability as:

$$g(s, p) = (1-p) \delta_{s,0} + p \sum_{s_1=0}^{\infty} \cdots \sum_{s_c=0}^{\infty} g_{cav}(s_1, p) \cdots g_{cav}(s_c, p) \delta_{s,1+s_1+\cdots+s_c}, \quad (21)$$

160 the only difference being that the product is over c terms g_{cav} , since all the c edges of the
 161 given site are present.

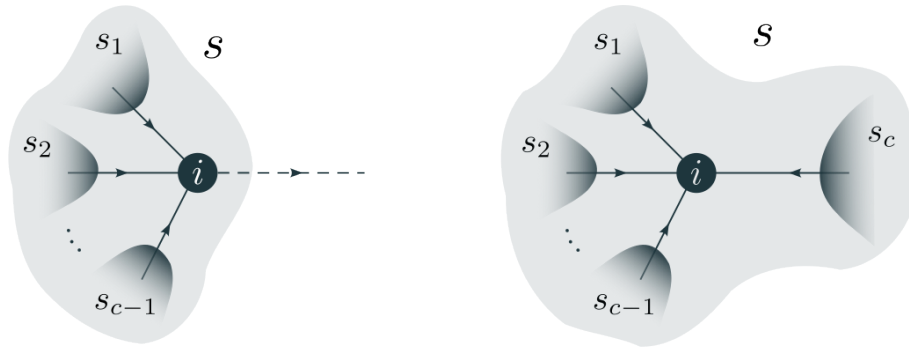


Figure 1: Graphic representation of Eqs. (20) and (21). Left: on a Bethe lattice with connectivity c one of the edges of site i is removed, represented with a dashed line. The $c-1$ remaining neighboring sites are connected by site i only, thus the probabilities $g_{cav}(s_1, p), \dots, g_{cav}(s_{c-1}, p)$ are factorized. The total resulting size is $s = 1 + s_1 + \cdots + s_{c-1}$. Right: in this case none of the edges of site i is removed. Again the cavity probabilities are factorized, but in this case the product includes $g_{cav}(s_c, p)$ too.

162 Next we define the generating function $\tilde{g}(t, p) \equiv \sum_{s=0}^{\infty} g(s, p) e^{-ts}$ and its cavity coun-
 163 terpart, $\tilde{g}_{cav}(t, p)$. Eq. (20) becomes:

$$\tilde{g}_{cav}(t, p) = (1-p) + p (\tilde{g}_{cav}(t, p))^{c-1} e^{-t}. \quad (22)$$

164 Deriving the above equation with respect to t and setting $t = 0$ we obtain

$$\tilde{g}'_{cav}(0, p) = \frac{p}{p(c-1) - 1}. \quad (23)$$

165 The moments of $g(s, p)$ are related to the derivatives of $\tilde{g}(t, p)$ in $t = 0$, in particular, recalling
 166 the definition (6) we have:

$$\chi_2(p) = -\tilde{g}'(0, p) = \frac{p(p+1)}{1-p(c-1)}, \quad (24)$$

167 that diverges, as expected, at the critical point $p_c = 1/(c-1)$. It is possible to obtain the
 168 previous divergent behavior considering the two-point correlation $C_2(\mathbf{x}_1, \mathbf{x}_2)$ defined in the
 169 previous Section. As we will see in Sec. 5, the correlation between two sites at distance L on
 170 the Bethe lattice is $C_2(|\mathbf{x}_1 - \mathbf{x}_2| = L) = p p^L$. The associated susceptibility, χ_2 , turns out to be

$$\chi_2 = \sum_{\mathbf{x}_2} C_2(|\mathbf{x}_1 - \mathbf{x}_2|) = p + p \sum_{L=1}^{\infty} c(c-1)^{L-1} p^L = \frac{p(p+1)}{1-p(c-1)}, \quad (25)$$

171 where the sum over \mathbf{x}_2 is over all the sites of the Bethe lattice and $c(c-1)^{L-1}$ is the number
 172 of neighboring sites at distance $L \geq 1$. We notice that in the Bethe lattice the two-point
 173 correlation is always exponentially decaying, also at the critical point $p = p_c$. The reason for
 174 the divergence is the number of neighboring sites which is exponential in the distance L . This
 175 means that the correlation length ξ_{BL} , implicitly defined by

$$C_2(L) \propto p^L \equiv e^{-\frac{L}{\xi_{BL}}} \quad (26)$$

176 is always finite and equal to $(-\log(p))^{-1}$. With this definition of ξ_{BL} the anomalous dimen-
 177 sion, η , associated to the power law behavior of $C_2(L)$, and the exponent ν associated to the
 178 power law behavior of the correlation length, are not defined on the Bethe lattice¹. One of
 179 the interesting features of the M -layer construction is that it allows to compute η and ν also
 180 in the limit $M \rightarrow \infty$, as we will discuss later.

181 **Scaling of $n(s, p)$** In order to compute the scaling of $n(s, p)$, we are interested in the func-
 182 tions $g(s, p)$ for p close to the critical point and s large, that corresponds to small values of t
 183 in $\tilde{g}(t, p)$. We now define

$$\delta\tilde{g}(t, p) \equiv \tilde{g}(t, p) - 1 = \sum_{s=0}^{\infty} g(s, p)(e^{-st} - 1) \quad (27)$$

184 and its cavity counterpart $\delta\tilde{g}_{cav}(t, p) \equiv \tilde{g}_{cav}(t, p) - 1$. Differentiating Eq. (22) with respect
 185 to t we obtain, for small values of t and p close to p_c :

$$\delta\tilde{g}'_{cav}(t, p)(1 - p/p_c - (c-2)\delta\tilde{g}_{cav}(t, p)) = -p_c, \quad (28)$$

186 from which we have

$$\delta\tilde{g}_{cav}(t, p) = a(1 - (1 + t/t^*)^{1/2}), \quad (29)$$

187 where

$$\delta p \equiv p - p_c \quad a \equiv -\delta p \frac{c-1}{c-2}, \quad t^* \equiv \delta p^2 \frac{(c-1)^3}{2c-4}. \quad (30)$$

188 For small values of t and δp we also obtain

$$\delta\tilde{g}(t, p) = \frac{c}{c-1} \delta\tilde{g}_{cav}(t, p). \quad (31)$$

189 Replacing the sum with an integral (which is justified by the fact that small values of t corre-
 190 spond to large values of s) we obtain, computing the inverse Laplace transform of Eq. (29)
 191 and using Eq. (31)

$$g(s, p) \sim \frac{1}{s^{3/2}} e^{-st^*} \rightarrow n(s, p) \sim \frac{1}{s^{5/2}} e^{-st^*}, \quad (32)$$

¹Notice that one can consider an alternative definition of ξ as $\xi^2 \equiv \frac{\sum_{\mathbf{x}_2} |\mathbf{x}_1 - \mathbf{x}_2|^2 C_2(\mathbf{x}_1, \mathbf{x}_2)}{\sum_{\mathbf{x}_2} C_2(\mathbf{x}_1, \mathbf{x}_2)}$ [1,2]. With this definition ξ is divergent on the Bethe lattice. This discrepancy is a pathology associated to the topology of the Bethe lattice in which the volume grows exponentially with the distance while it grows as a power law in finite dimension. In finite dimension this discrepancy is not present and indeed we will choose the second definition.

192 that obeys Eq. (4) with exponents

$$\sigma = \frac{1}{2} \quad \text{and} \quad \tau = \frac{5}{2}, \quad (33)$$

193 that we identify with the mean-field values. In the next Sections we will consider percolation
 194 on the M -layer random lattice in finite dimension D . In the limit $M \rightarrow \infty$ the function
 195 $n(\mathbf{s}, \mathbf{p})$ of the M -layer becomes identical to that of the Bethe lattice and therefore $\tau = 5/2$
 196 and $\sigma = 1/2$. In addition, we will show that for $M \rightarrow \infty$ the two-point function obeys the
 197 scaling form (1) with exponents

$$\nu = \frac{1}{2}, \quad \eta = 0, \quad (34)$$

198 in all dimensions $D \geq 2$, see the comment after Eq. (64). Note that these relationships are
 199 consistent with (7) and (8) only for $D = D_U = 6$. Indeed $\tau = D/D_f + 1$ is a hyperscaling
 200 relationship that is not generically valid [22] at variance with the more general $\sigma^{-1} = \nu D_f$,
 201 which implies $D_f = 4$ for the $M \rightarrow \infty$ model in any dimension. Computing the $1/M$ correc-
 202 tions around the $M \rightarrow \infty$ limit, we will show that for M finite the critical exponents are the
 203 same of the $M \rightarrow \infty$ limit for $D \geq D_U = 6$ while they are different for $D < D_U = 6$. On the
 204 other hand for $D < 6$ both relationships (7) and (8) hold. We note that the $M \rightarrow \infty$ model
 205 plays essentially the role of the Gaussian model in ferromagnetism, see [20], Chaps. 4 and 5.

206 4 The M -layer expansion

207 Conceptually the M -layer method is rather straightforward: 1) one introduces a D -dimensional
 208 random lattice depending on a parameter M , the limit $M \rightarrow \infty$ of the model is solvable as
 209 it coincides with the Bethe lattice solution; 2) then one computes the finite- M corrections in
 210 powers of $1/M$ around the Bethe lattice solution. The goal is to study the critical behaviour
 211 near a second order phase transition for a model on a given lattice and, as we anticipated in
 212 Section 2, from the $1/M$ expansion one can obtain the ϵ -expansion. The M -layer expansion
 213 has been introduced in Ref. [12] where diagrammatic rules were derived to compute $1/M$ cor-
 214 rections, in this Section we recall these rules, referring to the original paper for their derivation
 215 and all the details. Note that percolation itself is particularly useful to understand the origin
 216 of these rules and it is treated as an example in Section D of Ref. [12].

217 One can build the so-called M -layer construction considering M different layers of the
 218 original model, and then rewiring the bonds between each nearest-neighboring node among
 219 the layers in such a way that each node on each layer still has the same number of neighbors,
 220 that now can be placed at different layers [24]. In the following we will focus on D -dimensional
 221 hyper-cubic lattices (for which the connectivity is $2D$), even if the M -layer construction can be
 222 applied to any type of lattice. We call “topological loop” a sequence of adjacent edges on the
 223 lattice that starts and ends in the same site. While finite dimensional lattices are characterized
 224 by the presence of many short topological loops, in the end of the procedure, the number of
 225 topological loops in the M -layer lattice will typically be reduced and in the $M \rightarrow \infty$ limit there
 226 will be no loops of finite length: the $M \rightarrow \infty$ solution of the model will correspond to the Bethe
 227 solution [19], computed on a random regular tree-like graph with the same fixed connectivity
 228 as the original model. At this point we can expand around this Bethe solution, introducing the
 229 small parameter $1/M$. The original model corresponds to $M = 1$, thus in principle one should
 230 need all orders in $1/M$ to obtain the correct solution for the original model. However, we are
 231 interested in the critical behaviour of the model, which should be independent of the actual
 232 value of M due to universality. This expectation will indeed be confirmed in the context of
 233 percolation by the present computation. Furthermore, this implies that at each order in the

234 $1/M$ expansion we only need to consider the contributions that diverge the most approaching
 235 the critical point. One can show that the $1/M$ expansion for a generic \mathbf{q} -point observable
 236 corresponds to an expansion in the number of topological loops considered when computing
 237 that observable. In the limit of large M , in a given realization of these random rewirings the
 238 \mathbf{q} sites considered for the observable will be connected with highest probability (proportional
 239 to $1/M$) by a sequence of adjacent edges (a “path”) without topological loops, with lower
 240 probability by a path containing one topological loop and so on. In order to average over the
 241 rewirings the sum over all the possible realizations is needed, but we can retain the larger
 242 (in powers of $1/M$) contributions. We will call the path connecting the \mathbf{q} sites on a given
 243 realization a “topological diagram”, that can contain an arbitrary number of topological loops,
 244 zero in the limit $M \rightarrow \infty$. In particular, if one wants to compute the $1/M$ expansion for a
 245 generic observable \mathcal{O} , the following steps are required:

- 246 • *Step 1: Identify the possible topological diagrams*

247 Depending on the order at which one wants to perform the expansion, one should iden-
 248 tify the possible topological diagrams over which one needs to compute the chosen ob-
 249 servable. If one is interested in the leading order, one should only look at diagrams
 250 without loops, that correspond to the Bethe locally tree-like topology. If one wants to
 251 compute the next-to-leading order, one has to identify all the possible topological dia-
 252 grams that correspond to a Bethe lattice in which it has been manually injected a single
 253 topological loop, while any additional topological loop inserted will bring a new factor
 254 $1/M$ in the expansion.

- 255 • *Step 2: Weights, number of projections and symmetry factors*

256 For any diagram \mathcal{G} identified in Step 1, one needs to associate to it:

- 257 – a weight $W(\mathcal{G})$, that will be a power of $1/M$ and will indicate the probability that
 258 a topological diagram of that kind is obtained in the rewiring procedure;
- 259 – a symmetry factor $S(\mathcal{G})$, completely equivalent to that introduced in field theory
 260 for Feynman diagrams [21], that takes into account the number of ways in which
 261 vertices and lines can be switched leaving the topological structure of the diagram
 262 unaltered, see appendix C of Ref. [12] for a more detailed explanation of the equiv-
 263 alence between $S(\mathcal{G})$ and Feynman diagrams symmetry factors;
- 264 – the number of realizations of the chosen topological diagram on the original lattice,
 265 $\mathcal{N}(\mathcal{G})$: just as an example, if the chosen diagram is a line of length L between two
 266 points \mathbf{x}_1 and \mathbf{x}_2 , the number of such diagrams in the M -layered lattice having
 267 a different projection on the original lattice corresponds to the number of non-
 268 backtracking paths (NBP) of length L between the two points and its analytical
 269 expression is known in the literature [12, 25]. One can define $\mathcal{N}_L(\mathbf{x}_1, \mathbf{x}_2, \hat{\mu}, \hat{\nu})$ as
 270 the number of NBP of length L where the directions $\hat{\mu}$ and $\hat{\nu}$ of the lines entering
 271 respectively in the external points \mathbf{x}_1 and \mathbf{x}_2 is fixed to one among the $2D$ possible
 272 ones. In the large L limit, the actual value of the number of NBP will be independent
 273 on those directions, and we will simply define this number as $\mathcal{N}_L(\mathbf{x}_1, \mathbf{x}_2)$. The
 274 total number of the simple line diagrams of length L between two points \mathbf{x}_1 and \mathbf{x}_2
 275 will thus be $\mathcal{N}(\mathcal{G}) = (2D)^2 \mathcal{N}_L(\mathbf{x}_1, \mathbf{x}_2)$, where the factor $(2D)^2$ counts the possible
 276 entering directions of the line in the two external points. If one has a more complex
 277 diagram, to identify $\mathcal{N}(\mathcal{G})$ it is sufficient to multiply a factor $\mathcal{N}_L(\mathbf{x}_i, \mathbf{x}_j)$ for each
 278 internal line of length L , a factor $2D$ for each external vertex and a factor $\frac{(2D)!}{(2D-k)!}$
 279 for any internal vertex of degree k , to count the different possible directions of the
 280 lines entering the vertex.

- 281 • *Step 3: Computation of the line-connected observable on the chosen diagram*

282 For any diagram \mathcal{G} identified in Step 1, one then needs to compute the value $\mathcal{O}(\mathcal{G})$ of the
 283 chosen observable computed on a Bethe lattice in which the topological structure of that
 284 diagram has been manually injected. This observable will depend on the topology of the
 285 diagram and on the length of the lines. In order to compute, for a given observable, the
 286 expansion in the number of loops, or equivalently in powers of $1/M$, one should isolate
 287 different contributions coming from a given topological diagram. Generically, the contri-
 288 bution of a diagram without loops is contained in the one coming from the same diagram
 289 with some additional lines composing a loop. For this purpose we want to subtract the
 290 first contribution from the one coming from the loop diagram, this amounts to compute
 291 the so-called “line-connected observable”, $\mathcal{O}_{lc}(\mathcal{G})$. For the diagrams considered in this
 292 paper the following operative definition is sufficient: in order to compute $\mathcal{O}_{lc}(\mathcal{G})$ one
 293 has to compute the observable on the given diagram \mathcal{G} and then subtract all the contri-
 294 butions from the observable computed on diagrams where a line composing the loop (if
 295 any) is removed. For a more detailed treatment the reader is referred to Ref. [12].

- 296 • *Step 4: Sum of the contributions*

297 At the end, we need to sum the contributions to the chosen observable coming from the
 298 different chosen diagrams. Because the values of the chosen observable only depend on
 299 the projection of the considered diagrams, for each diagram \mathcal{G} , we multiply the value
 300 of the line-connected observable $\mathcal{O}_{lc}(\mathcal{G})$ by $\mathcal{N}(\mathcal{G})$, $\mathcal{S}(\mathcal{G})$, $\mathcal{W}(\mathcal{G})$, and we sum over the
 301 positions of internal vertices and over the lengths of the internal lines.

302 5 M -layer for percolation in D dimensions

303 In this Section we apply the procedure described in the previous Section to the percolation
 304 problem. We consider both the problems of site and bond percolation on a hypercubic lattice
 305 in D dimensions, which we denote $\mathbf{a}_l \mathbb{Z}^D$, considering \mathbf{a}_l the lattice spacing. Following the
 306 notation of Sec. 2 we define p (where $0 < p \leq 1$) as the probability that a site or an edge is
 307 present, for the case of site or bond percolation respectively. Since the M -layer approach is a
 308 way to construct an expansion for observables around the Bethe solution, we define the “bare
 309 mass”

$$\mu \equiv -\ln\left(\frac{p}{p_c}\right) \quad \text{for } p \sim p_c, \quad (35)$$

310 where $p_c = 1/(2D - 1)$ is the critical value for both site and bond percolation on a Bethe
 311 lattice with branching ratio $2D - 1$, above which the so-called “giant cluster” is present.

312 Following the prescriptions of the M -layer construction [12, 24] we report here the results
 313 of the application to both percolation problems in the non-percolating phase, $p < p_c$. We
 314 are interested in two observables: the two and three-point correlation functions $\mathcal{C}_2(\mathbf{x}_1, \mathbf{x}_2)$
 315 and $\mathcal{C}_3(\mathbf{x}_1, \mathbf{x}_2, \mathbf{x}_3)$, where $\overline{\cdot}$ denotes the average over the rewirings of the M -layer procedure.
 316 According to the M -layer rules these correlation functions will be written as sums, over dif-
 317 ferent diagrams, of $\mathcal{C}_{n,lc}(\mathcal{G}; \{\mathcal{L}\})$, the n -point line-connected correlation, averaged over the
 318 realizations of the percolation problem and computed on the diagram \mathcal{G} , embedded on a tree
 319 graph, where $\{\mathcal{L}\}$ indicates the lengths of the different lines of the diagram. For both site
 320 and bond percolation, the two-point (three-point) correlation is defined as the probability
 321 that two (three) sites, at positions \mathbf{x}_1 and \mathbf{x}_2 ($\mathbf{x}_1, \mathbf{x}_2$ and \mathbf{x}_3) are occupied and belong to the
 322 same cluster. In the end, at one loop level, we must subtract pieces already considered in
 323 loop-free diagrams, to compute the “line-connected” observable [12, 24]. We analyse the two
 324 observables separately, following for each of them the steps listed in the previous Section.

325 **Observable:** $\overline{C_2(\mathbf{x}_1, \mathbf{x}_2)}$

326 • Step 1: *Identify the possible topological diagrams*

327 The simplest diagram connecting two points is the bare line, which we will call \mathcal{G}_1 . Includ-
 328 ing the possibility of a loop to be present we consider the diagram composed of four lines with
 329 two vertices of degree three, where the two internal lines compose a loop. We will call this
 330 diagram \mathcal{G}_2 .

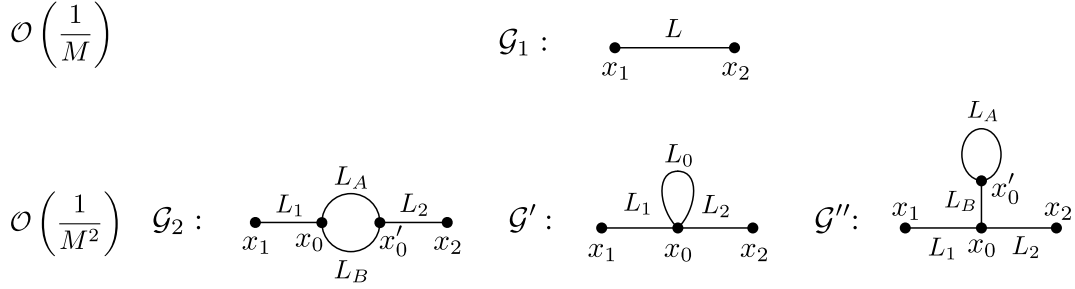


Figure 2: Diagrams that contribute to the two-point correlation functions up to one loop.

331 Other possibilities are the tadpole-type diagrams, connecting two points with a loop gen-
 332 erated by one four-degree vertex or connecting two points by two three-degree vertices, re-
 333 spectively the diagrams \mathcal{G}' and \mathcal{G}'' in Fig. 2. Nevertheless, these last two diagrams give no
 334 contributions to the *line-connected* two-point observable for percolation, as we will see in Step
 335 3 below. We won't consider them in the following steps.

336 • Step 2: *Weights, number of projections and symmetry factors*

337 Diagram \mathcal{G}_1 :

338 ♦ $W(\mathcal{G}_1) = \frac{1}{M}$;

339 ♦ $\mathcal{N}(\mathcal{G}_1; L; \mathbf{x}_1, \mathbf{x}_2) = (2D)^2 \mathcal{N}_L(\mathbf{x}_1, \mathbf{x}_2)$;

340 ♦ $S(\mathcal{G}_1) = 1$.

341 Diagram \mathcal{G}_2 :

342 ♦ $W(\mathcal{G}_2) = \frac{1}{M^2}$;

343 ♦ $\mathcal{N}(\mathcal{G}_2; \vec{L}; \mathbf{x}_1, \mathbf{x}_2) = (2D)^2 \left(\frac{(2D)!}{(2D-3)!} \right)^2 \sum_{\mathbf{x}_0, \mathbf{x}'_0} \mathcal{N}_{L_1}(\mathbf{x}_1, \mathbf{x}_0) \mathcal{N}_{L_2}(\mathbf{x}'_0, \mathbf{x}_2) \prod_{i=A,B} \mathcal{N}_{L_i}(\mathbf{x}_0, \mathbf{x}'_0)$;

344 ♦ $S(\mathcal{G}_2) = 2$.

345 where $\vec{L} = (L_1, L_A, L_B, L_2)$.

346 • Step 3: *Computation of $C_{2,lc}(\mathcal{G}_1; L)$ and $C_{2,lc}(\mathcal{G}_2; \vec{L})$*

347 Given the definition of the line-connected two-point correlation for both percolation prob-
 348 lems, we firstly compute the contributions of diagrams \mathcal{G}_1 and \mathcal{G}_2 for the problem of site per-
 349 colation:

350
$$C_{2,lc}(\mathcal{G}_1; L) = p p^L; \tag{36}$$

$$C_{2,lc}(\mathcal{G}_2; \vec{L}) = -p^{L_1+L_2+L_A+L_B}. \tag{37}$$

351 The first result is immediate since, in the non-percolating phase, all the $L + 1$ sites, connected
 352 by a line of length L , must be active, in order to connect the two sites at the extremities.
 353 The second result appears because, for the sites at the extremities to be connected, one or

354 both lines of the loop must consist on active sites, in addition to the external lines, which
 355 also need to be composed of active sites. The associated probability for this to happen is
 356 $p^{L_1+1}(p^{L_A-1} + p^{L_B-1} - p^{L_A+L_B-2})p^{L_2+1}$. The aforementioned result is obtained subtracting
 357 the straight line contributions, already taken into account with \mathcal{G}_1 : $p^{L_1+1}p^{L_A-1}p^{L_2+1}$ and
 358 $p^{L_1+1}p^{L_B-1}p^{L_2+1}$. This last operation is the application of the ‘‘line-connected’’ definition [12].

359 Performing the same computation for diagrams \mathcal{G}' and \mathcal{G}'' we obtain zero, as anticipated.
 360 The reason is that the two tadpoles, that enter the site \mathbf{x}_0 , do not change the probability that
 361 sites \mathbf{x}_1 and \mathbf{x}_2 belong to the same cluster with respect to the case where the loop is not present.
 362 Indeed, independently of the lines of the tadpole, site \mathbf{x}_0 must be active in order to connect the
 363 two sites, then, subtracting the contributions needed to define the line-connected observable,
 364 that are the simple lines without tadpoles, the net contribution is zero. These diagrams are
 365 instead relevant in the percolating phase that we aim to study in a subsequent work.

366 A similar computation can be performed for the bond percolation. In this case, consider-
 367 ing the contribution of \mathcal{G}_1 , in order for the two sites to be in the same cluster, all the edges
 368 connecting the two must be active:

$$C_{2,lc}^{bond}(\mathcal{G}_1; \mathbf{L}) = p^L; \quad (38)$$

369 Similarly, the line-connected contribution for \mathcal{G}_2 , is

$$C_{2,lc}^{bond}(\mathcal{G}_2; \vec{\mathbf{L}}) = -p^{L_1+L_2+L_A+L_B}. \quad (39)$$

370 The same argument, used for the site percolation problem, can be applied to the topological
 371 diagrams \mathcal{G}' and \mathcal{G}'' in the bond percolation case, for which they give zero contribution too.

372 • Step 4: *Sum of the contributions*

373 The expression for $\overline{C_2(\mathbf{x}_1, \mathbf{x}_2)}$, that is for the site percolation, is

$$\begin{aligned} \overline{C_2(\mathbf{x}_1, \mathbf{x}_2)} &= \frac{1}{M} \sum_{\mathbf{L}} \mathcal{N}(\mathcal{G}_1; \mathbf{L}; \mathbf{x}_1, \mathbf{x}_2) C_{2,lc}(\mathcal{G}_1; \mathbf{L}) + \\ &+ \frac{1}{2M^2} \sum_{\vec{\mathbf{L}}} \mathcal{N}(\mathcal{G}_2; \vec{\mathbf{L}}; \mathbf{x}_1, \mathbf{x}_2) C_{2,lc}(\mathcal{G}_2; \vec{\mathbf{L}}) + \mathcal{O}\left(\frac{1}{M^3}\right), \end{aligned} \quad (40)$$

374 while, for the bond percolation problem, we have

$$\begin{aligned} \overline{C_2^{bond}(\mathbf{x}_1, \mathbf{x}_2)} &= \frac{1}{M} \sum_{\mathbf{L}} \mathcal{N}(\mathcal{G}_1; \mathbf{L}; \mathbf{x}_1, \mathbf{x}_2) C_{2,lc}^{bond}(\mathcal{G}_1; \mathbf{L}) + \\ &+ \frac{1}{2M^2} \sum_{\vec{\mathbf{L}}} \mathcal{N}(\mathcal{G}_2; \vec{\mathbf{L}}; \mathbf{x}_1, \mathbf{x}_2) C_{2,lc}^{bond}(\mathcal{G}_2; \vec{\mathbf{L}}) + \mathcal{O}\left(\frac{1}{M^3}\right). \end{aligned} \quad (41)$$

375 We can notice that the only difference is for the observable computed on a given diagram, here
 376 \mathcal{G}_1 and \mathcal{G}_2 , which is the only model dependent part of the M -layer computations.

377 **Observable:** $\overline{C_3(\mathbf{x}_1, \mathbf{x}_2, \mathbf{x}_3)}$

378 • Step 1: *Identify the possible topological diagrams*

379 The simplest diagram connecting three points is the bare three-degree vertex, which we will
 380 call \mathcal{G}_3 . Including the possibility for a loop to be present, we consider the diagram, composed
 381 of six lines, with three vertices of degree three, we will call this diagram \mathcal{G}_4 . At one-loop
 382 level there are three more diagrams connecting three points with a single loop, which are the
 383 same as \mathcal{G}_3 , but where one of the external legs is dressed with \mathcal{G}_2 . We call such a diagram \mathcal{G}_5 ,
 384 including all the permutations. All these diagrams are reported in Fig. 3.

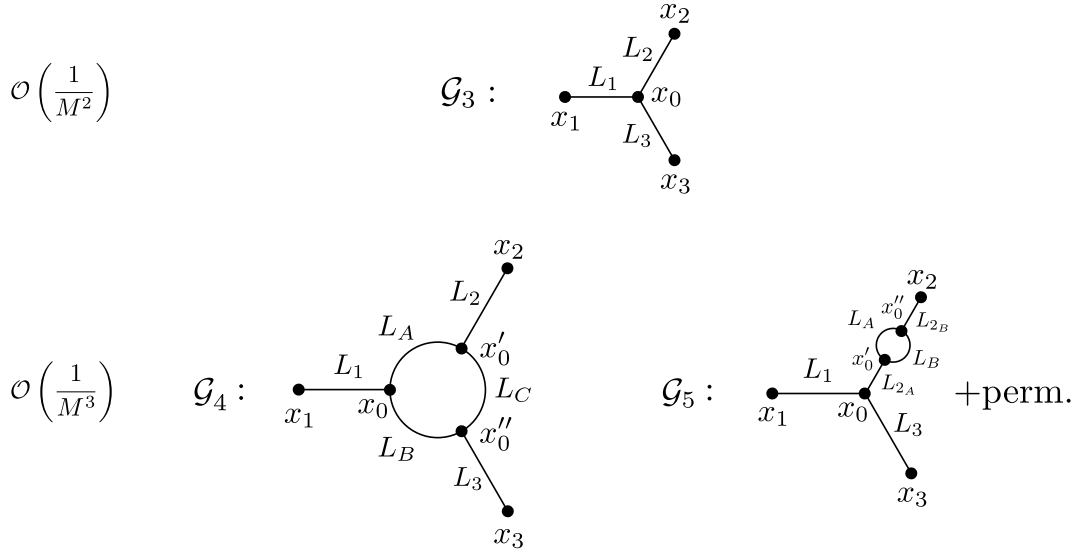


Figure 3: Diagrams that contribute to the three-point correlation functions up to one loop.

- Step 2: *Weights, number of projections and symmetry factors*

Diagram \mathcal{G}_3 :

◆ $W(\mathcal{G}_3) = \frac{1}{M^2};$

◆ $\mathcal{N}(\mathcal{G}_3; \vec{L}'; \mathbf{x}_1, \mathbf{x}_2, \mathbf{x}_3) = (2D)^3 \frac{(2D)!}{(2D-3)!} \sum_{x_0} \prod_{i=1}^3 \mathcal{N}_{L_i}(\mathbf{x}_i, \mathbf{x}_0);$

◆ $S(\mathcal{G}_3) = 1.$

Diagram \mathcal{G}_4 :

◆ $W(\mathcal{G}_4) = \frac{1}{M^3};$

◆ $\mathcal{N}(\mathcal{G}_4; \vec{L}''; \mathbf{x}_1, \mathbf{x}_2, \mathbf{x}_3) = (2D)^3 \left(\frac{(2D)!}{(2D-3)!} \right)^3 \times$
 $\sum_{x_0, x'_0, x''_0} \mathcal{N}_{L_1}(\mathbf{x}_1, \mathbf{x}_0) \mathcal{N}_{L_2}(\mathbf{x}_2, \mathbf{x}'_0) \mathcal{N}_{L_3}(\mathbf{x}_3, \mathbf{x}''_0) \mathcal{N}_{L_A}(\mathbf{x}_0, \mathbf{x}'_0) \mathcal{N}_{L_B}(\mathbf{x}_0, \mathbf{x}''_0) \mathcal{N}_{L_C}(\mathbf{x}'_0, \mathbf{x}''_0);$

◆ $S(\mathcal{G}_4) = 1.$

Diagram \mathcal{G}_5 :

◆ $W(\mathcal{G}_5) = \frac{1}{M^3};$

◆ $\mathcal{N}(\mathcal{G}_5; \vec{L}'''; \mathbf{x}_1, \mathbf{x}_2, \mathbf{x}_3) = (2D)^3 \left(\frac{(2D)!}{(2D-3)!} \right)^3 \times$
 $\sum_{x_0, x'_0, x''_0} \mathcal{N}_{L_1}(\mathbf{x}_1, \mathbf{x}_0) \mathcal{N}_{L_{2_A}}(\mathbf{x}_0, \mathbf{x}'_0) \mathcal{N}_{L_{2_B}}(\mathbf{x}_2, \mathbf{x}''_0) \mathcal{N}_{L_3}(\mathbf{x}_3, \mathbf{x}_0) \prod_{i=A,B} \mathcal{N}_{L_i}(\mathbf{x}'_0, \mathbf{x}''_0);$

◆ $S(\mathcal{G}_5) = 2,$

where $\vec{L}' = (L_1, L_2, L_3)$, $\vec{L}'' = (\vec{L}', L_A, L_B, L_C)$ and $\vec{L}''' = (L_1, L_{2_A}, L_B, L_{2_B}, L_3)$.

- Step 3: *Computation of $\mathcal{C}_{3,lc}(\mathcal{G}_3; \vec{L}')$, $\mathcal{C}_{3,lc}(\mathcal{G}_4; \vec{L}''')$ and $\mathcal{C}_{3,lc}(\mathcal{G}_5; \vec{L}''')$*

As for the two-point function we compute the contributions, starting from the site percolation problem:

$$\mathcal{C}_{3,lc}(\mathcal{G}_3; \vec{L}') = p p^{L_1+L_2+L_3}; \quad (42)$$

$$404 \quad C_{3,lc}(\mathcal{G}_4; \vec{L}'') = -2p^{L_1+L_2+L_3+L_A+L_B+L_C}; \quad (43)$$

$$405 \quad C_{3,lc}(\mathcal{G}_5; \vec{L}''') = -p^{L_1+L_{2A}+L_{2B}+L_A+L_B+L_3}. \quad (44)$$

406 The result for \mathcal{G}_3 is easily derived, considering that all the sites of the topology must be active
 407 for the extremities to be connected. The result for \mathcal{G}_5 is obtained by multiplying the contri-
 408 bution for the bare vertex by the loop correction of the two-point function, diagram \mathcal{G}_2 , with
 409 the corresponding lengths. The contribution of \mathcal{G}_4 is a generalization of the computation for
 410 \mathcal{G}_2 ; to connect the three extremities two of the three (or all the three) lines of the loop must
 411 consist on all active sites. Moreover, in this case we have to subtract three contributions, cor-
 412 responding to cutting L_A , L_B , and L_C respectively, already included in the bare contribution
 413 \mathcal{G}_3 .

414 Analogously to the two-point function, we use the same arguments to compute the contri-
 415 butions for the bond percolation three-point function:

$$C_{3,lc}^{bond}(\mathcal{G}_3; \vec{L}') = p^{L_1+L_2+L_3}; \quad (45)$$

$$416 \quad C_{3,lc}^{bond}(\mathcal{G}_4; \vec{L}'') = -2p^{L_1+L_2+L_3+L_A+L_B+L_C}; \quad (46)$$

$$417 \quad C_{3,lc}^{bond}(\mathcal{G}_5; \vec{L}''') = -p^{L_1+L_{2A}+L_{2B}+L_A+L_B+L_3}. \quad (47)$$

418 • Step 4: *Sum of the contributions*

419 The expression for $C_3(\mathbf{x}_1, \mathbf{x}_2, \mathbf{x}_3)$, that is for the site percolation, is

$$\begin{aligned} \overline{C_3(\mathbf{x}_1, \mathbf{x}_2, \mathbf{x}_3)} &= \frac{1}{M^2} \sum_{\vec{L}'} \mathcal{N}(\mathcal{G}_3; \vec{L}'; \mathbf{x}_1, \mathbf{x}_2, \mathbf{x}_3) C_{3,lc}(\mathcal{G}_3; \vec{L}') + \\ &+ \frac{1}{M^3} \sum_{\vec{L}''} \mathcal{N}(\mathcal{G}_4; \vec{L}''; \mathbf{x}_1, \mathbf{x}_2, \mathbf{x}_3) C_{3,lc}(\mathcal{G}_4; \vec{L}'') + \\ &+ \frac{1}{2M^3} \sum_{\vec{L}'''} \mathcal{N}(\mathcal{G}_5; \vec{L}'''; \mathbf{x}_1, \mathbf{x}_2, \mathbf{x}_3) C_{3,lc}(\mathcal{G}_5; \vec{L}''') + \mathcal{O}\left(\frac{1}{M^4}\right). \end{aligned} \quad (48)$$

420 As noticed for the two-point function, the expression is of $\overline{C_3^{bond}(\mathbf{x}_1, \mathbf{x}_2, \mathbf{x}_3)}$, that is for the bond
 421 percolation, is the same as $\overline{C_3(\mathbf{x}_1, \mathbf{x}_2, \mathbf{x}_3)}$ with the corresponding observables: $C_{3,lc}^{bond}(\mathcal{G}_3; \vec{L}')$,
 422 $C_{3,lc}^{bond}(\mathcal{G}_4; \vec{L}'')$ and $C_{3,lc}^{bond}(\mathcal{G}_5; \vec{L}''')$. We do not write it for brevity.

423 In appendix C we discuss why we didn't include other possible but *irrelevant* diagrams to
 424 study the critical behavior of the percolation problem and in appendix D we present the explicit
 425 computation of the leading order critical behaviour of the four-point correlation function.

426 **Computation of the moments of $n(s, p)$** In order to compute χ_2 and χ_3 we Fourier trans-
 427 form $\overline{C_2(\mathbf{x}_1, \mathbf{x}_2)}$ and $\overline{C_3(\mathbf{x}_1, \mathbf{x}_2, \mathbf{x}_3)}$, given in Eqs. (40) and (48), using the following conven-
 428 tion:

$$\widehat{h}(\mathbf{k}) = a_l^D \sum_{\mathbf{x} \in a_l \mathbb{Z}^D} h(\mathbf{x}) e^{i\mathbf{k}\mathbf{x}}, \quad h(\mathbf{x}) = \int_{[-\frac{\pi}{a_l}, \frac{\pi}{a_l}]} \frac{d^D \mathbf{k}}{(2\pi)^D} \widehat{h}(\mathbf{k}) e^{-i\mathbf{k}\mathbf{x}}; \quad (49)$$

429 that implies

$$\left(\frac{2\pi}{a_l}\right)^D \delta^D(\mathbf{k}) = \sum_{\mathbf{x} \in a_l \mathbb{Z}^D} e^{i\mathbf{k}\mathbf{x}}. \quad (50)$$

430 We also use the fact that $\mathcal{N}_L(\mathbf{x}_1, \mathbf{x}_2)$ is a function of the difference between the starting and
431 arrival point only, so that, in Fourier space, we have

$$\widehat{\mathcal{N}}_L(\mathbf{k}_1, \mathbf{k}_2) = (2\pi)^D \delta(\mathbf{k}_1 + \mathbf{k}_2) \widehat{\mathcal{N}}_L(\mathbf{k}_1) \quad (51)$$

432 where, for small \mathbf{k} [12, 15],

$$\widehat{\mathcal{N}}_L(\mathbf{k}) \approx 2D(2D-1)^{L-1} a_l^D e^{-k^2 a_l^2 L/(2D-2)}. \quad (52)$$

433 In view of the fact that in the critical region the sums will be dominated by large L contribu-
434 tions, we may write the sums over the lengths as integrals:

$$\sum_{L=1}^{\infty} \rightarrow \int_{1/\Lambda^2}^{\infty} dL, \quad (53)$$

435 where we introduced the UV cutoff $\Lambda = 1$ to make contact with field theory. Note that while in
436 field-theory the UV cutoff is inserted manually, in the M -layer construction it arises naturally
437 due to the lattice spacing (see more details in appendix B). The resulting expressions, for the
438 site percolation case, of the two and three-point functions are respectively

$$\begin{aligned} \overline{\widehat{\mathcal{C}}_2(\mathbf{k}, \mathbf{k}')} &= \frac{\widehat{C} \widehat{B}^2 a_l^D}{\widehat{A} \mu} \frac{1}{\widehat{k}^2 + 1} (2\pi)^D \delta^D(\mathbf{k} + \mathbf{k}') \times \\ &\left(1 - \frac{\widehat{A} \mu^{\frac{D}{2}-3}}{2(\widehat{k}^2 + 1)} \int \frac{d^D \widehat{\mathbf{q}}}{(2\pi)^D} \int d\widehat{L}_A d\widehat{L}_B e^{-(1+(\widehat{k}-\widehat{q})^2)\widehat{L}_A} e^{-(1+\widehat{q}^2)\widehat{L}_B} \right) + \mathcal{O}\left(\frac{1}{M^3}\right) \end{aligned} \quad (54)$$

439 and

$$\begin{aligned} \overline{\widehat{\mathcal{C}}_3(\mathbf{k}_1, \mathbf{k}_2, \mathbf{k}_3)} &= \frac{\widehat{C} \widehat{B}^3 a_l^{2D}}{\widehat{A} \mu^3} \frac{(2\pi)^D \delta^D(\mathbf{k}_1 + \mathbf{k}_2 + \mathbf{k}_3)}{(\widehat{k}_1^2 + 1)(\widehat{k}_2^2 + 1)(\widehat{k}_3^2 + 1)} \times \\ &\left(1 - 2\widehat{A} \mu^{\frac{D}{2}-3} \int \frac{d^D \widehat{\mathbf{q}}}{(2\pi)^D} \int d\widehat{L}_A d\widehat{L}_B d\widehat{L}_C e^{-(1+(\widehat{k}_2+\widehat{k}_3+\widehat{q})^2)\widehat{L}_A} e^{-(1+(\widehat{k}_2+\widehat{q})^2)\widehat{L}_B} e^{-(1+\widehat{q}^2)\widehat{L}_C} + \right. \\ &\left. - \frac{1}{2} \frac{\widehat{A} \mu^{\frac{D}{2}-3}}{(\widehat{k}_2 + \widehat{k}_3)^2 + 1} \int \frac{d^D \widehat{\mathbf{q}}}{(2\pi)^D} \int d\widehat{L}_A d\widehat{L}_B e^{-(1+(\widehat{k}_2+\widehat{q})^2)\widehat{L}_A} e^{-(1+\widehat{q}^2)\widehat{L}_B} + \text{perm.} \right) + \mathcal{O}\left(\frac{1}{M^4}\right), \end{aligned} \quad (55)$$

440 where μ is the one defined in Eq. (35). We also defined the following non-universal constants:

$$\widehat{A} \equiv \frac{1}{M} \left(\frac{(2D)!}{(2D-3)!} \right)^2 p^{-1} (2D-2)^{\frac{D}{2}} \left(\frac{2D}{2D-1} \right)^3, \quad (56)$$

$$\widehat{B} \equiv \frac{1}{M} 2D \left(\frac{(2D)!}{(2D-3)!} \right) \left(\frac{2D}{2D-1} \right)^2, \quad (57)$$

$$\widehat{C} \equiv (2D-2)^{\frac{D}{2}}, \quad (58)$$

441 and we rescaled the momenta and lengths according to:

$$\widehat{\mathbf{k}} \equiv \mathbf{k} \frac{a_l}{\sqrt{\mu(2D-2)}}, \quad \text{and} \quad \widehat{L}_i \equiv L_i \mu. \quad (59)$$

442 Note that in Eqs. (54), (55) we have omitted the the extremes of integration ($\mu/\Lambda^2, \infty$) of
443 the integrals over \widehat{L} . In appendix A we show how to generalize this kind of computation for a

444 V_e -point function, with $V_e \geq 2$, moreover we explain the reasoning behind the identification
 445 of the constants \widehat{A} , \widehat{B} and \widehat{C} . The same steps can be done for the bond percolation problem,
 446 the only difference being the definition of the non-universal constant \widehat{A} :

$$\widehat{A}_{bond} \equiv \frac{1}{M} \left(\frac{(2D)!}{(2D-3)!} \right)^2 (2D-2)^{\frac{D}{2}} \left(\frac{2D}{2D-1} \right)^3, \quad (60)$$

447 in which no factor p^{-1} appears, at variance with Eq. (56). In the following we will perform
 448 explicit computations for the site problem only, the reader can reproduce them for the bond
 449 percolation simply using Eq. (60) instead of Eq. (56).

450 In appendix B we show that the above expression, for $\widehat{C}_2(\mathbf{k}, \mathbf{k}')$ and $\widehat{C}_3(\mathbf{k}_1, \mathbf{k}_2, \mathbf{k}_3)$, are
 451 precisely the same that appear from the Feynman diagrams of the corresponding scalar cubic
 452 field-theory obtained from the Fortuin-Kasteleyn mapping to the $n+1$ -state Potts model in the
 453 limit $n \rightarrow 0$, corresponding to percolation [6–9].

454 From the above expressions we compute the functions χ_q introduced in Section 2. Notice
 455 that we did not rescale the momenta inside the momentum conservation delta functions, thus,
 456 to compute χ_q , according to Eq. (5), we have simply to divide by $\alpha_l^{(q-1)D}$, remove $(2\pi)^D$ times
 457 the conservation delta function and set the external momenta to zero. This leads to

$$\chi_2(\mu) = \frac{\widehat{C}\widehat{B}^2}{\widehat{A}\mu} \left(1 - \frac{\widehat{A}\mu^{\frac{D}{2}-3}}{2(4\pi)^{\frac{D}{2}}} \int \frac{d\widehat{L}_A d\widehat{L}_B}{(\widehat{L}_A + \widehat{L}_B)^{\frac{D}{2}}} e^{-\widehat{L}_A - \widehat{L}_B} \right) + \mathcal{O}\left(\frac{1}{M^3}\right), \quad (61)$$

458

$$\begin{aligned} \chi_3(\mu) = \frac{\widehat{C}\widehat{B}^3}{\widehat{A}\mu^3} \left(1 - \frac{2\widehat{A}\mu^{\frac{D}{2}-3}}{(4\pi)^{\frac{D}{2}}} \int \frac{d\widehat{L}_A d\widehat{L}_B d\widehat{L}_C}{(\widehat{L}_A + \widehat{L}_B + \widehat{L}_C)^{\frac{D}{2}}} e^{-\widehat{L}_A - \widehat{L}_B - \widehat{L}_C} + \right. \\ \left. - \frac{3\widehat{A}\mu^{\frac{D}{2}-3}}{2} \int \frac{d\widehat{L}_A d\widehat{L}_B}{(\widehat{L}_A + \widehat{L}_B)^{\frac{D}{2}}} e^{-\widehat{L}_A - \widehat{L}_B} \right) + \mathcal{O}\left(\frac{1}{M^4}\right). \end{aligned} \quad (62)$$

459 **Ginzburg criterion for D_U** Once the two-point function is computed, in this paper using the
 460 M -layer construction, it is possible to deduce the upper critical dimension of the problem, D_U ,
 461 applying the Ginzburg criterion in the non-critical phase [26]. We first introduce the function
 462 $\widehat{G}(\mathbf{k})$, corresponding to the *propagator* in the field-theoretical language, as

$$\widehat{C}_2(\mathbf{k}, \mathbf{k}') \equiv (2\pi)^D \delta^D(\mathbf{k} + \mathbf{k}') \widehat{G}(\mathbf{k}). \quad (63)$$

463 Using this definition, together with Eq. (54), we have

$$\begin{aligned} \widehat{G}(\mathbf{k}) \propto \frac{1}{M} \frac{1}{\rho k^2 + \mu} \times \\ \left(1 - \frac{1}{M} \frac{\mathbf{c}}{\rho k^2 + \mu} \int \frac{d^D q}{(2\pi)^D} \sum_{L_A, L_B=1}^{\infty} e^{-(\rho(k-q)^2 + \mu)L_A} e^{-(\rho q^2 + \mu)L_B} \right) + \mathcal{O}\left(\frac{1}{M^3}\right), \end{aligned} \quad (64)$$

464 where we rescaled momenta and lengths according to Eq. (59), with $\rho \equiv a_l^2/(2D-2)$ and
 465 $\mathbf{c} \equiv M\widehat{A}/2$ defined in order to make the $1/M$ factors explicit. Notice that we also made
 466 use of the relation in Eq. (53) to write sums instead of integrals. Here we understand that
 467 for $M \rightarrow \infty$ the correction can be neglected and the two-point function assumes the mean-
 468 field expression, *i.e.* the Gaussian propagator, which leads to the mean-field values for the
 469 anomalous dimension, $\eta = 0$, and the exponent associated to the correlation length, $\nu = 1/2$.

470 Moreover, in high dimensions we expect for the two-point function the following Gaussian
471 form near the critical point and for $k^2 \rightarrow 0$

$$(M\widehat{G}(k))^{-1} \propto \mathcal{A}(\mu - \mu_c) + \mathcal{B}\rho k^2 + \mathcal{O}(k^4), \quad (65)$$

472 from which we have the correction, at order $1/M$, to the control parameter

$$\mu_c = -\frac{c}{M} \frac{1}{(4\pi\rho)^{\frac{D}{2}}} \sum_{L_A, L_B=1}^{\infty} \frac{1}{(L_A + L_B)^{\frac{D}{2}}} \quad (66)$$

473 and the two prefactors

$$\mathcal{A} = 1 - \frac{c}{M} \frac{1}{(4\pi\rho)^{\frac{D}{2}}} \sum_{L_A, L_B=1}^{\infty} \frac{1}{(L_A + L_B)^{\frac{D}{2}-1}}, \quad (67)$$

474

$$\mathcal{B} = 1 - \frac{c}{M} \frac{1}{(4\pi\rho)^{\frac{D}{2}}} \sum_{L_A, L_B=1}^{\infty} \frac{L_A L_B}{(L_A + L_B)^{\frac{D}{2}+1}}. \quad (68)$$

475 We notice that these three corrections, μ_c , \mathcal{A} and \mathcal{B} , diverge respectively for $D \leq 4$, $D \leq 6$
476 and $D \leq 6$, revealing that the upper critical dimension for the site percolation problem, where
477 the mean-field behavior breaks down, is $D_U = 6$. Again we notice that the analysis doesn't
478 change considering bond percolation, since the only difference is in the definition of the factor
479 c , not relevant for these divergences. In order to go below the upper critical dimension we can
480 rewrite the propagator, including the cutoff in the integrals as prescribed by Eq. (53):

$$(M\widehat{G}_2(k))^{-1} \propto \mu(\widehat{k}^2 + 1) \times \left(1 + \frac{c}{M} \frac{\mu^{\frac{D}{2}-3}}{(\widehat{k}^2 + 1)} \frac{1}{(4\pi)^{D/2}} \int_{\mu/\Lambda^2}^{\infty} d\widehat{L}_A d\widehat{L}_B \frac{1}{(L_A + L_B)^{\frac{D}{2}}} e^{-\widehat{L}_A - \widehat{L}_B - \widehat{k}^2 \frac{L_A L_B}{L_A + L_B}} \right) + \mathcal{O}\left(\frac{1}{M^3}\right). \quad (69)$$

481 We understand that the correction is not negligible for $D < 6$ in the limit $\mu \rightarrow 0$, due to the
482 presence of the term $\mu^{\frac{D}{2}-3}$. Moreover the integrals over L_A and L_B diverge in the ultraviolet
483 (UV) regime, that is for $\mu/\Lambda^2 \rightarrow 0$ if $D \geq 4$ and in particular for $D \simeq 6$ from below. In
484 order for the integrals to be finite in the limit $\mu/\Lambda^2 \rightarrow 0$ we should perform the standard
485 mass renormalization, changing variable from μ to $m^2 \equiv \xi^{-2}$, to be explicitly done in the next
486 Section.

487 6 Computation of critical exponents

488 In this Section we start from the results of the M -layer construction for the two and three-point
489 observables and we perform standard procedures in order to compute the ϵ -expansion for the
490 critical exponents. From the definition of $\widehat{G}(k)$, Eq. (63) we can define the correlation length
491 ξ :

$$\xi^2 \equiv \widehat{G}(0) \frac{\partial \widehat{G}^{-1}(k)}{\partial k^2} \Big|_{k^2=0}, \quad (70)$$

492 where, with a little abuse of notation, we identify with k the modulus of the corresponding
493 vector. Since

$$\frac{\partial}{\partial k^2} = \frac{\partial \widehat{k}^2}{\partial k^2} \frac{\partial}{\partial \widehat{k}^2} = \frac{a_l^2}{\mu \widehat{c}^{\frac{2}{D}}} \frac{\partial}{\partial \widehat{k}^2} \quad (71)$$

494 we have:

$$\widehat{G}(0) = \frac{\widehat{C}\widehat{B}^2 a_l^D}{\widehat{A}\mu} \left(1 - \frac{\widehat{A}\mu^{\frac{D}{2}-3}}{2(4\pi)^{\frac{D}{2}}} \int \frac{d\widehat{L}_A d\widehat{L}_B}{(\widehat{L}_A + \widehat{L}_B)^{\frac{D}{2}}} e^{-\widehat{L}_A - \widehat{L}_B} \right), \quad (72)$$

495 and for small \widehat{A} (that is for large M):

$$\widehat{G}^{-1}(k) \simeq \frac{\widehat{A}\mu}{\widehat{C}\widehat{B}^2 a_l^D} \left(\widehat{k}^2 + 1 + \frac{\widehat{A}\mu^{\frac{D}{2}-3}}{2(4\pi)^{\frac{D}{2}}} \int \frac{d\widehat{L}_a d\widehat{L}_b}{(\widehat{L}_a + \widehat{L}_b)^{\frac{D}{2}}} e^{-\frac{\widehat{L}_a \widehat{L}_b}{\widehat{L}_a + \widehat{L}_b} \widehat{k}^2 - \widehat{L}_a - \widehat{L}_b} \right), \quad (73)$$

496 where in the r.h.s. we have replaced k with \widehat{k} according to the definition given in (59). We
497 then obtain:

$$\left. \frac{\partial \widehat{G}^{-1}(k)}{\partial \widehat{k}^2} \right|_{\widehat{k}^2=0} = \frac{\widehat{A}\mu}{\widehat{C}\widehat{B}^2 a_l^D} \left(1 + \frac{\widehat{A}\mu^{\frac{D}{2}-3}}{2(4\pi)^{\frac{D}{2}}} \int \frac{d\widehat{L}_a d\widehat{L}_b}{(\widehat{L}_a + \widehat{L}_b)^{\frac{D}{2}}} e^{-\widehat{L}_a - \widehat{L}_b} \frac{\partial}{\partial \widehat{k}^2} \left(e^{-\frac{\widehat{L}_a \widehat{L}_b}{\widehat{L}_a + \widehat{L}_b} \widehat{k}^2} \right) \right|_{\widehat{k}^2=0} \right), \quad (74)$$

498 where

$$\int \frac{d\widehat{L}_a d\widehat{L}_b}{(\widehat{L}_a + \widehat{L}_b)^{\frac{D}{2}}} e^{-\widehat{L}_a - \widehat{L}_b} \frac{\partial}{\partial \widehat{k}^2} \left(e^{-\frac{\widehat{L}_a \widehat{L}_b}{\widehat{L}_a + \widehat{L}_b} \widehat{k}^2} \right) \Big|_{\widehat{k}^2=0} = - \int \frac{d\widehat{L}_a d\widehat{L}_b}{(\widehat{L}_a + \widehat{L}_b)^{\frac{D}{2}+1}} \widehat{L}_a \widehat{L}_b e^{-\widehat{L}_a - \widehat{L}_b}. \quad (75)$$

499 We want to notice that in Eqs. (72), (73) and (74) we neglected higher orders, with respect
500 to the one-loop corrections, in powers of $1/M$. From now on we will neglect these terms if
501 not explicitly specified. Defining

$$I_\alpha(\mu) \equiv \int_{\mu/\Lambda^2}^{\infty} d\widehat{L}_a d\widehat{L}_b \frac{e^{-\widehat{L}_a - \widehat{L}_b}}{(\widehat{L}_a + \widehat{L}_b)^{\frac{D}{2}}} \quad (76)$$

502 and

$$I_\beta(\mu) \equiv \int_{\mu/\Lambda^2}^{\infty} d\widehat{L}_a d\widehat{L}_b \frac{\widehat{L}_a \widehat{L}_b}{(\widehat{L}_a + \widehat{L}_b)^{\frac{D}{2}+1}} e^{-\widehat{L}_a - \widehat{L}_b}, \quad (77)$$

503 we have

$$\xi^2(\mu) = \frac{1}{m^2(\mu)} = \frac{a_l^2}{\widehat{C}^{\frac{2}{D}} \mu} \left(1 - \frac{1}{2} \frac{\widehat{A}\mu^{\frac{D}{2}-3}}{(4\pi)^{\frac{D}{2}}} \left(I_\alpha(\mu) + I_\beta(\mu) \right) \right). \quad (78)$$

504 In the integrals in Eqs. (76), (77), we have written explicitly the extremes of integration that
505 we have omitted previously. Notice that the integral $I_\alpha(\mu)$ is UV divergent in $D = 6$ for $\mu \rightarrow 0$
506 (i.e., $p \rightarrow p_c$). Now we can simply invert the relation, to express μ as a function of m^2 :

$$\mu(m^2) = a_l^2 \widehat{C}^{-\frac{2}{D}} m^2 \left(1 - \frac{1}{2} \frac{\widehat{A} m^{D-6} \widehat{C}^{\frac{6}{D}-1} a_l^{D-6}}{(4\pi)^{\frac{D}{2}}} \left(I_\alpha(\mu(m^2)) + I_\beta(\mu(m^2)) \right) \right). \quad (79)$$

507 Notice that the previous equations for χ_2 and χ_3 are written as functions of μ , which is not
508 the ‘‘physical mass’’, thus they can be divergent, for $\mu \rightarrow 0$, near the upper critical dimension,
509 $D_U = 6$. To avoid the divergences we need the expression of μ as a function of m^2 , to correctly
510 write λ , as defined in Eq. (83). To this aim we compute $\xi^2(\mu)$ (and so $m^2(\mu)$) from its
511 definition.

512 At this point we have all the ingredients to write χ_2 and χ_3 as functions of the physical
513 parameter m^2 . Plugging Eq. (79) into Eqs. (61) and (62) we obtain:

$$\begin{aligned}
\chi_2(m^2) &= \frac{\widehat{C}\widehat{B}^2\widehat{C}^{\frac{2}{D}}}{\widehat{A}a_l^2} m^{-2} \left(1 + \frac{1}{2} \frac{\widehat{A}m^{D-6}\widehat{C}^{\frac{6}{D}-1}a_l^{D-6}}{(4\pi)^{\frac{D}{2}}} \left(I_\alpha(\mu(m^2)) + I_\beta(\mu(m^2)) \right) \right) \times \\
&\quad \times \left(1 - \frac{1}{2} \frac{\widehat{A}m^{D-6}\widehat{C}^{\frac{6}{D}-1}a_l^{D-6}}{(4\pi)^{\frac{D}{2}}} I_\alpha(\mu(m^2)) \right) \\
&= \frac{\widehat{C}\widehat{B}^2\widehat{C}^{\frac{2}{D}}}{\widehat{A}a_l^2} m^{-2} \left(1 + \frac{1}{2} \frac{\widehat{A}m^{D-6}\widehat{C}^{\frac{6}{D}-1}a_l^{D-6}}{(4\pi)^{\frac{D}{2}}} I_\beta(\mu(m^2)) \right), \quad (80)
\end{aligned}$$

$$\begin{aligned}
\chi_3(m^2) &= \frac{\widehat{C}\widehat{B}^3\widehat{C}^{\frac{6}{D}}}{\widehat{A}a_l^6} m^{-6} \left(1 + \frac{3}{2} \frac{\widehat{A}m^{D-6}\widehat{C}^{\frac{6}{D}-1}a_l^{D-6}}{(4\pi)^{\frac{D}{2}}} \left(I_\alpha(\mu(m^2)) + I_\beta(\mu(m^2)) \right) \right) \times \\
&\quad \times \left(1 - 2 \frac{\widehat{A}m^{D-6}\widehat{C}^{\frac{6}{D}-1}a_l^{D-6}}{(4\pi)^{\frac{D}{2}}} I_\gamma(\mu(m^2)) - \frac{3}{2} \frac{\widehat{A}m^{D-6}\widehat{C}^{\frac{6}{D}-1}a_l^{D-6}}{(4\pi)^{\frac{D}{2}}} I_\alpha(\mu(m^2)) \right) \\
&= \frac{\widehat{C}\widehat{B}^3\widehat{C}^{\frac{6}{D}}}{\widehat{A}a_l^6} m^{-6} \left(1 + \frac{\widehat{A}m^{D-6}\widehat{C}^{\frac{6}{D}-1}a_l^{D-6}}{(4\pi)^{\frac{D}{2}}} \left(\frac{3}{2} I_\beta(\mu(m^2)) - 2I_\gamma(\mu(m^2)) \right) \right), \quad (81)
\end{aligned}$$

514 where

$$I_\gamma(\mu) \equiv \int_{\mu/\Lambda^2}^{\infty} d\widehat{L}_A d\widehat{L}_B d\widehat{L}_C \frac{e^{-\widehat{L}_A - \widehat{L}_B - \widehat{L}_C}}{(\widehat{L}_A + \widehat{L}_B + \widehat{L}_C)^{\frac{D}{2}}}. \quad (82)$$

515 Notice that $\chi_2(\mu)$ and $\chi_3(\mu)$ have UV divergences near 6 dimensions due the presence of
516 $I_\alpha(\mu)$, which disappears when they are written as functions of m , i.e. $\chi_2(m^2)$ and $\chi_3(m^2)$
517 are free of UV divergences near 6 dimensions.

518 **Critical exponents in fixed dimension** In this Section we perform the fixed-dimension com-
519 putation of the critical exponents [20]. Led by the scaling laws discussed in Sec. 2, we compute
520 the following dimensionless ratio:

$$\lambda \equiv \left(\frac{a_l}{\xi} \right)^D \frac{\chi_3^2(m^2)}{\chi_2^3(m^2)}. \quad (83)$$

521 On the other hand m^2 is connected to the bare distance from the critical point by

$$m^2 \sim |\mu - \mu_c|^{2\nu} \quad \text{and} \quad \xi \sim |\mu - \mu_c|^{-\nu}, \quad (84)$$

522 where ν is the critical exponent for the divergence of the correlation length. In the end,
523 defining

$$u \equiv \widehat{A}\widehat{C}^{\frac{6}{D}-1}a_l^{D-6} m^{D-6} \equiv g m^{D-6}, \quad (85)$$

524 we can compute the ratio λ

$$\lambda = u \left(1 - 2 \frac{u}{(4\pi)^{\frac{D}{2}}} \left(-\frac{3}{4} I_\beta(\mu(m^2)) + 2I_\gamma(\mu(m^2)) \right) \right). \quad (86)$$

525 Note that λ depends on the microscopic parameters of the model only through the single
 526 parameter $u = \mathcal{O}(1/M)$. Now we can compute the integrals I_β and I_γ in the limit $m^2 \rightarrow 0$,
 527 which are convergent near $D = 6$:

$$\lim_{m^2 \rightarrow 0} I_\beta(\mu(m^2)) = \frac{1}{6} \Gamma\left(3 - \frac{D}{2}\right), \quad (87)$$

528

$$\lim_{m^2 \rightarrow 0} I_\gamma(\mu(m^2)) = \frac{1}{2} \Gamma\left(3 - \frac{D}{2}\right). \quad (88)$$

529 Thus in the limit $m^2 \rightarrow 0$

$$\lambda = u - \frac{7}{4} \frac{u^2}{(4\pi)^{\frac{D}{2}}} \Gamma\left(3 - \frac{D}{2}\right), \quad (89)$$

530 from which

$$u \simeq \lambda + \frac{7}{4} \frac{\lambda^2}{(4\pi)^{\frac{D}{2}}} \Gamma\left(3 - \frac{D}{2}\right). \quad (90)$$

531 Now, following the standard procedure (see Ref. [20], Chap. 8), we define the function $\mathbf{b}(\lambda)$
 532 as:

$$\mathbf{b}(\lambda) \equiv m^2 \frac{\partial}{\partial m^2} \Big|_{g \text{ fixed}} \lambda = \frac{1}{2}(D-6)u \frac{\partial}{\partial u} \Big|_{m^2 \text{ fixed}} \lambda = \frac{1}{2}(D-6) \left(u - \frac{7}{2} \frac{u^2}{(4\pi)^{\frac{D}{2}}} \Gamma\left(3 - \frac{D}{2}\right) \right). \quad (91)$$

533 From Eq. (90) we obtain:

$$\mathbf{b}(\lambda) = \frac{1}{2}(D-6) \left(\lambda - \frac{7}{4} \frac{\lambda^2}{(4\pi)^{\frac{D}{2}}} \Gamma\left(3 - \frac{D}{2}\right) \right). \quad (92)$$

534 We constructed λ to be a dimensionless quantity that does not diverge at the critical point. For
 535 this reason, we can identify the critical value of λ as the point at which the function $\mathbf{b}(\lambda)$ is
 536 zero, as we discussed in Sec. 2. While a trivial zero is always present at $\lambda = 0$, for $D < 6$ we
 537 see that there also exists a non-trivial zero:

$$\lambda_c = \frac{4}{7} \frac{(4\pi)^{\frac{D}{2}}}{\Gamma\left(3 - \frac{D}{2}\right)}. \quad (93)$$

538 As already remarked in Sec. 2, the value of λ_c is universal, in the sense that it is no more
 539 dependent on the specific value of g , and thus on the specific problem we are considering,
 540 bond or site percolation. From this point the computation is really the same for the two cases,
 541 realizing universality between these two versions of the percolation problem.

542 Remembering that $m^2 \sim (\mu - \mu_c)^{2\nu}$, following standard computations [20], we define:

$$z(\lambda) \equiv \frac{\partial \mu}{\partial m^2} \sim m^{2D_1}, \quad (94)$$

543 where $D_1 = \frac{1}{2\nu} - 1$. We can thus compute it as:

$$D_1(\lambda) \equiv m^2 \frac{\partial}{\partial m^2} \Big|_{g \text{ fixed}} \ln(z(\lambda)). \quad (95)$$

544 In the same way, for the computation of η we need to define:

$$D_2(\lambda) \equiv \frac{\partial \ln \chi_2}{\partial \ln m^2} \Big|_{g \text{ fixed}}, \quad \chi_2 \sim m^{2\frac{\eta-2}{2}}, \quad D_2(\lambda_c) = -1 + \frac{\eta}{2}. \quad (96)$$

545 We start from the computation of \mathbf{z} :

$$\mathbf{z}(\lambda) = \alpha_l^2 \widehat{G}^{-\frac{2}{D}} \left(1 - \frac{1}{2} \frac{u}{(4\pi)^{\frac{D}{2}}} \frac{D-4}{2} I_\beta(\mu(m^2)) - \frac{1}{2} \frac{g}{(4\pi)^{\frac{D}{2}}} \frac{\partial}{\partial m^2} \left(m^{D-4} I_\alpha(\mu(m^2)) \right) \right) \quad (97)$$

546 where

$$\frac{\partial}{\partial m^2} \left(m^{D-4} I_\alpha(\mu(m^2)) \right) = -m^{D-6} \int_{\mu(m^2)/\Lambda^2}^{\infty} d\widehat{L}_a d\widehat{L}_b \frac{e^{-\widehat{L}_a - \widehat{L}_b}}{(\widehat{L}_a + \widehat{L}_b)^{\frac{D}{2}-1}} \equiv -m^{D-6} I'_\alpha(\mu(m^2)). \quad (98)$$

547 We can compute I'_α :

$$\lim_{m^2 \rightarrow 0} I'_\alpha(\mu(m^2)) = \Gamma\left(3 - \frac{D}{2}\right), \quad (99)$$

548 obtaining

$$\mathbf{z}(\lambda) \propto 1 - \frac{u}{2} \frac{1}{(4\pi)^{\frac{D}{2}}} \Gamma\left(3 - \frac{D}{2}\right) \frac{D-16}{12}, \quad (100)$$

549 and, from the definition of $D_1(\lambda)$, we arrive at the critical exponent ν in D dimensions:

$$\nu_D = \frac{42}{84 + (6-D)(D-16)}. \quad (101)$$

550 The next exponent, η , requires the computation of $D_2(\lambda)$

$$D_2(\lambda) \equiv \left. \frac{\partial \ln \chi_2}{\partial \ln m^2} \right|_{g \text{ fixed}} = \frac{m^2}{\chi_2} \left. \frac{\partial \chi_2}{\partial m^2} \right|_{g \text{ fixed}} = -1 + \frac{\lambda}{2} \frac{1}{(4\pi)^{\frac{D}{2}}} I_\beta(\mu(m^2)) \left(\frac{D}{2} - 3 \right), \quad (102)$$

551 which can be obtained using

$$\begin{aligned} \left. \frac{\partial \chi_2}{\partial m^2} \right|_{g \text{ fixed}} &\propto -m^{-4} + \frac{1}{2} \frac{u}{(4\pi)^{\frac{D}{2}}} m^{-4} I_\beta(\mu(m^2)) \frac{D-8}{2} \\ &= -m^{-4} \left(1 - \frac{1}{2} \frac{u}{(4\pi)^{\frac{D}{2}}} I_\beta(\mu(m^2)) \frac{D-8}{2} \right), \end{aligned} \quad (103)$$

552

$$\chi_2 \propto m^{-2} \left(1 + \frac{1}{2} \frac{u}{(4\pi)^{\frac{D}{2}}} I_\beta(\mu(m^2)) \right), \quad (104)$$

553 from which we have

$$\eta_D = \frac{D-6}{21}. \quad (105)$$

554 **ϵ -expansion** Given the results of Eqs. (101) and (105) in fixed dimension we can perform
555 the computation in $D = 6 - \epsilon$:

$$\nu = \frac{1}{2} + \frac{5}{84} \epsilon + \mathcal{O}(\epsilon^2), \quad (106)$$

556

$$\eta = -\frac{1}{21} \epsilon + \mathcal{O}(\epsilon^2). \quad (107)$$

557 These results are, to first order in ϵ , equal to the expansion of the standard field theory asso-
558 ciated with the percolation problem [3, 6, 8–11].

559 7 Conclusion

560 In this article we have shown how to recover, at one-loop level of approximation, the results
 561 of the ϵ -expansion for the critical exponents of the percolation problem on a D -dimensional
 562 regular lattice, by means of a new method, the M -layer construction. To do so, we computed
 563 the observables of interest for the case of site percolation in the non-percolating phase — the
 564 two- and three-point correlation functions, i.e. the probability that two or three sites belong
 565 to the same cluster — in properly chosen graphs at the leading orders. We then computed
 566 the ϵ -expansion for the critical exponents, recovering, at first order, the same values already
 567 obtained for bond percolation using the $n \rightarrow 0$ continuation of the field theory applied to the
 568 Potts model with $n + 1$ states. Moreover, we have shown that within the M -layer construction
 569 the bond percolation problem differs from site percolation only for non-universal constants,
 570 which directly implies the universality between site and bond percolation in any dimension D .
 571 The analysis presented here clearly illustrates that the M -layer construction effectively allows
 572 one to extract quantitative information on the critical behavior even for problems which are
 573 not defined by a Hamiltonian, such as percolation.

574 We explained for the first time how this method can be applied to a known problem in
 575 order to obtain the ϵ -expansion of the critical exponents. Recent studies have used the M -
 576 layer construction to derive non-trivial insights into models whose critical behavior is not yet
 577 completely understood [14–18], or to show that for well-known problems the one-loop results
 578 align with those from standard field theory [13, 24]. In this paper, we push this approach a
 579 step forward by showing how, applying the standard theoretical recipes of the renormalization
 580 group, one can extract the series for the critical exponents. We believe that this investigation
 581 could be highly beneficial in guiding the computation of critical exponents for problems where
 582 the standard RG approach is inapplicable [18].

583 Regarding the specific problem of percolation, it would be interesting to extend the calcu-
 584 lations made in this work to the percolating phase $p > p_c$. In this sense, the preliminary cal-
 585 culation of the Ginzburg criterion at the bare order (i.e. without loops) has already been done
 586 using the M -layer construction, obtaining the known upper critical dimension, $D_U = 6$ [27].
 587 To proceed further and obtain the values of the critical exponents in the percolating phase,
 588 it is necessary to calculate the same observables as Ref. [27] with the corrections due to the
 589 one-loop structures. We leave this analysis to future work.

590 A Identification of the constants in the M -layer expansion

591 In this Section we generalize the computation of the main text for the two and three-point
 592 function, with the goal of identifying the least number of constants that describe the loop
 593 expansion in the M -layer framework. In particular we will perform the computations for both
 594 site and bond percolation problems, highlighting the differences between the two. Starting
 595 with the site percolation, we write all the contributions, in Fourier space, of a generic V_e -point
 596 correlation, computed on a generic topology, \mathcal{G} , with I lines, V_e external points, V_i internal
 597 vertices, N_{loop} number of loops:

$$\begin{aligned} \overline{\widehat{C}_{V_e}(\{k_j\})} \Big|_{\mathcal{G}} &= \frac{(2D)^{V_e}}{S(\mathcal{G}) M^{N_{loop} + V_e - 1}} \left(\frac{(2D)!}{(2D - 3)!} \right)^{V_i} \left(\prod_{i=1}^I \int dL_i \right) (2\pi)^D \delta^D \left(\sum_{j=1}^{V_e} k_j \right) \times \\ & \alpha_l^{-DV_i} \left(\int \prod_{l=1}^{N_{loop}} \frac{d^D q_l}{(2\pi)^D} \right) \left(\prod_{i=1}^I \widehat{\mathcal{N}}_{L_i}(\{q_l\}, \{k_j\}) \right) p^{I - 2V_i} f(C_{V_e, lc}) p^{\sum_{i=1}^I L_i}, \quad (\text{A.1}) \end{aligned}$$

598 with the same convention for the Fourier transform used in the main text, Eq. (49). Notice that
 599 \widehat{N}_L are functions of linear combinations $\mathbf{g}_i(\{\mathbf{q}_l\}, \{\mathbf{k}_j\})$ of internal ($\{\mathbf{q}_l\}$ for $l = 1, \dots, N_{loop}$)
 600 and external momenta ($\{\mathbf{k}_j\}$ for $j = 1, \dots, V_e$), that ensure momentum conservation at each
 601 vertex. The factor \mathbf{p}^{I-2V_i} and the function $f(C_{V_e,lc})$ come from Eqs. (36), (37), (42), (43)
 602 and (44). The first is the eventual extra factor \mathbf{p} , which is present only for $C_{2,lc}(\mathcal{G}_1; L)$ and
 603 $C_{3,lc}(\mathcal{G}_3; \vec{L}')$, as can be checked by substituting the corresponding values for I and V_i (notice
 604 that the specific expression, \mathbf{p}^{I-2V_i} , is valid only for three-degree vertices, for V_i d -degree
 605 vertices it is $\mathbf{p}^{I-(d-1)V_i}$ and can be generalized if vertices of different degree are present). The
 606 same goes for the factor $(2D-3)!$, whose generalization for a d -degree vertex is $(2D-d)!$.
 607 The function $f(C_{V_e,lc})$ assumes the following values:

$$f(C_{2,lc}(\mathcal{G}_1; L)) = 1, \quad (\text{A.2})$$

$$608 \quad f(C_{2,lc}(\mathcal{G}_2; \vec{L})) = -1, \quad (\text{A.3})$$

$$609 \quad f(C_{3,lc}(\mathcal{G}_3; \vec{L}')) = 1, \quad (\text{A.4})$$

$$610 \quad f(C_{3,lc}(\mathcal{G}_4; \vec{L}'')) = -2, \quad (\text{A.5})$$

$$611 \quad f(C_{3,lc}(\mathcal{G}_5; \vec{L}''')) = -1. \quad (\text{A.6})$$

612 Notice that the diagrams we computed in this work are of the form of Eq. (A.1). We believe
 613 that higher order diagrams (with three-degree vertices only) for a generic V_e -point function
 614 obey it as well, but this hypothesis is not necessary for the results described in this paper.
 615 In principle we should repeat all the steps done from Eq. (A.1) to Eq. (A.6) for the bond
 616 percolation problem. Generalizing the arguments given in Sec. 5, we notice that the only
 617 difference with respect to the site percolation problem is the factor \mathbf{p}^{I-V_i} in Eq. (A.1), which
 618 is not present for bond percolation.

619 Let us continue with site percolation. Using the asymptotic expression of the NBP in Fourier
 620 space, Eq. (52), together with the rescaling of momenta and lengths, in Eq. (59), we arrive at

$$\begin{aligned} \overline{\widehat{C}_{V_e}(\{\mathbf{k}_j\})} \Big|_{\mathcal{G}} &= \frac{(2D)^{V_e}}{S(\mathcal{G}) M^{N_{loop}-1+V_e}} \left(\frac{(2D)!}{(2D-3)!} \right)^{V_i} \mu^{-I} \left(\prod_{i=1}^I \int d\widehat{L}_i \right) \times \\ &\quad (2\pi)^D \delta^D \left(\sum_{j=1}^{V_e} \mathbf{k}_j \right) a_l^{-DV_i} \left(\int \prod_{l=1}^{N_{loop}} \frac{d^D \widehat{q}_l}{(2\pi)^D} \right) p^{I-2V_i} f(C_{V_e,lc}) \times \\ &\quad \left(\frac{\mu(2D-2)}{a_l^2} \right)^{\frac{D}{2}(N_{loop}-1)} \left(\frac{\mu(2D-2)}{a_l^2} \right)^{\frac{D}{2}} \left(\frac{2D}{2D-1} \right)^I \prod_{i=1}^I e^{-\mathbf{g}_i(\{\widehat{q}_l\}, \{\widehat{k}_j\})^2 \widehat{L}_i - \widehat{L}_i} a_l^{ID}, \quad (\text{A.7}) \end{aligned}$$

621 where $\widehat{\mathbf{k}}$ is a function of \mathbf{k} according to (59). Note that, as done in the main text, we did not
 622 rescale the external momenta inside the delta function.

623 Given the known relations for V_i , V_e , I and N_{loop} in a generic diagram with internal
 624 vertices of degree three:

$$V_i = V_e + 2(N_{loop} - 1) \quad \text{and} \quad I = 2V_e + 3(N_{loop} - 1), \quad (\text{A.8})$$

625 in Eq. (A.7) we can identify the following topology-dependent term:

$$\frac{1}{S(\mathcal{G})} \left(\prod_{i=1}^I \int d\widehat{L}_i \right) \left(\int \prod_{l=1}^{N_{loop}} \frac{d^D \widehat{q}_l}{(2\pi)^D} \right) f(C_{V_e,lc}) \prod_{i=1}^I e^{-\mathbf{g}_i(\{\widehat{q}_l\}, \{\widehat{k}_j\})^2 \widehat{L}_i - \widehat{L}_i} \quad (\text{A.9})$$

626 and the following three factors:

627 • a constant to the power $(N_{loop} - 1)$:

$$\frac{1}{M} \left(\frac{(2D)!}{(2D-3)!} \right)^2 p^{-1} (2D-2)^{\frac{D}{2}} \left(\frac{2D}{2D-1} \right)^3 \mu^{\frac{D}{2}-3} \equiv \widehat{A} \mu^{\frac{D}{2}-3}, \quad (\text{A.10})$$

628 • a constant to the power V_e :

$$\frac{1}{M} 2D \left(\frac{(2D)!}{(2D-3)!} \right) \left(\frac{2D}{2D-1} \right)^2 a_l^D \mu^{-2} \equiv \widehat{B} a_l^D \mu^{-2}, \quad (\text{A.11})$$

629 • an overall factor:

$$(2\pi)^D \delta^D \left(\sum_{j=1}^{V_e} k_j \right) \left(\frac{\mu(2D-2)}{a_l^2} \right)^{\frac{D}{2}} \equiv (2\pi)^D \delta^D \left(\sum_{j=1}^{V_e} k_j \right) \mu^{D/2} \widehat{C} a_l^{-D}, \quad (\text{A.12})$$

630 as defined in Eqs. (56), (57) and (58). Again we notice that the same expressions are obtained
631 in the bond percolation case, the only different one is the definition of \widehat{A} , given in this case by
632 (60).

633 With the expression given in Eq. (A.7) it is possible to easily identify the relevant constants
634 to perform the expansion in inverse powers of M . Let us remark that these are all non-universal
635 quantities, being the critical exponents independent from them.

636 B Connection with field theoretical expressions

637 In this Section we show how to write the expressions for $\widehat{C}_{2,lc}(k, k')$ and $\widehat{C}_{3,lc}(k_1, k_2, k_3)$,
638 Eqs. (54) and (55), in terms of scalar propagators, as in the corresponding field theory. To do
639 so, starting from the mentioned equations, we first perform the integrals over the lengths with
640 lower and upper limits of integration respectively μ/Λ^2 and ∞ . Notice that we are interested
641 in the critical behavior, that is for $\mu \rightarrow 0$, thus we can set the lower limit to 0, which amounts
642 to neglecting higher orders in μ . The results are

$$\begin{aligned} \widehat{C}_2(k, k') &= \frac{\widehat{C} \widehat{B}^2 a_l^D}{\widehat{A} \mu} \frac{1}{\widehat{k}^2 + 1} (2\pi)^D \delta^D(k + k') \times \\ &\quad \left(1 - \frac{\widehat{A} \mu^{\frac{D}{2}-3}}{2(\widehat{k}^2 + 1)} \int \frac{d^D \widehat{q}}{(2\pi)^D} \frac{1}{1 + (\widehat{k} - \widehat{q})^2} \frac{1}{1 + \widehat{q}^2} \right) + \mathcal{O}\left(\frac{1}{M^3}\right), \quad (\text{B.1}) \end{aligned}$$

$$\begin{aligned} \widehat{C}_3(k_1, k_2, k_3) &= \frac{\widehat{C} \widehat{B}^3 a_l^{2D}}{\widehat{A} \mu^3} \frac{(2\pi)^D \delta^D(k_1 + k_2 + k_3)}{(\widehat{k}_1^2 + 1)(\widehat{k}_2^2 + 1)(\widehat{k}_3^2 + 1)} \times \\ &\quad \left(1 - 2\widehat{A} \mu^{\frac{D}{2}-3} \int \frac{d^D \widehat{q}}{(2\pi)^D} \frac{1}{1 + (\widehat{k}_2 + \widehat{k}_3 + \widehat{q})^2} \frac{1}{1 + (\widehat{k}_2 + \widehat{q})^2} \frac{1}{1 + \widehat{q}^2} + \right. \\ &\quad \left. - \frac{1}{2} \frac{\widehat{A} \mu^{\frac{D}{2}-3}}{(\widehat{k}_2 + \widehat{k}_3)^2 + 1} \int \frac{d^D \widehat{q}}{(2\pi)^D} \frac{1}{1 + (\widehat{k}_2 + \widehat{q})^2} \frac{1}{1 + \widehat{q}^2} + \text{perm.} \right) + \mathcal{O}\left(\frac{1}{M^4}\right). \quad (\text{B.2}) \end{aligned}$$

643 Next we rescale the momenta and we define the bare mass and coupling, respectively m_b and
644 g_b , according to:

$$\widetilde{k} \equiv \mu^{\frac{1}{2}} a_l^{\frac{2D}{D+2}} \widehat{A}^{\frac{1}{D+2}} \widehat{B}^{-\frac{2}{D+2}} \widehat{k} \quad (\text{B.3})$$

645

$$m_b^2 \equiv \mu \alpha_l^{-\frac{4D}{D+2}} \widehat{A}^{\frac{2}{D+2}} \widehat{B}^{-\frac{4}{D+2}} \quad (\text{B.4})$$

646

$$g_b \equiv \alpha_l^D \widehat{A}^{\frac{D-6}{D+2}} \widehat{B}^{\frac{4}{D+2}} \widehat{C}^{-2+\frac{3}{D}+\frac{D}{4}} \quad (\text{B.5})$$

647 and we obtain

$$\begin{aligned} \overline{\widehat{C}_2(\tilde{k}, \tilde{k}')} &= (2\pi)^D \delta^D(k+k') \times \\ &\left(\frac{1}{\tilde{k}^2 + m_b^2} - \frac{1}{2} g_b^2 \frac{1}{(\tilde{k}^2 + m_b^2)^2} \int \frac{d^D \tilde{q}}{(2\pi)^D} \frac{1}{(\tilde{k} - \tilde{q})^2 + m_b^2} \frac{1}{\tilde{q}^2 + m_b^2} \right) + \mathcal{O}\left(\frac{1}{M^3}\right) \end{aligned} \quad (\text{B.6})$$

$$\begin{aligned} \overline{\widehat{C}_3(k_1, k_2, k_3)} &= \frac{1}{(\tilde{k}_1^2 + m_b^2)(\tilde{k}_2^2 + m_b^2)(\tilde{k}_3^2 + m_b^2)} (2\pi)^D \delta^D(\tilde{k}_1 + \tilde{k}_2 + \tilde{k}_3) \times \\ &\left(g_b - 2g_b^3 \int \frac{d^D \tilde{q}}{(2\pi)^D} \frac{1}{(\tilde{k}_2 + \tilde{k}_3 + \tilde{q})^2 + m_b^2} \frac{1}{(\tilde{k}_2 + \tilde{q})^2 + m_b^2} \frac{1}{\tilde{q}^2 + m_b^2} + \right. \\ &\left. - \frac{1}{2} g_b^3 \frac{1}{(\tilde{k}_2 + \tilde{k}_3)^2 + m_b^2} \int \frac{d^D \tilde{q}}{(2\pi)^D} \frac{1}{(\tilde{k}_2 + \tilde{q})^2 + m_b^2} \frac{1}{\tilde{q}^2 + m_b^2} + \text{perm.} \right) + \mathcal{O}\left(\frac{1}{M^4}\right), \end{aligned} \quad (\text{B.7})$$

648 which are the results of the corresponding field theory associated with the percolation problem
649 [7, 9].

650 As a last remark we notice that it is not always possible to write the results of the M -layer
651 construction in terms of scalar propagators. For the percolation problem, the observables
652 computed on a given topology, such as Eqs. (36) or (37), are powers of the probability p to
653 some combination of the lengths of the lines, thus the integrals over the lengths give the scalar
654 propagator factors. For a generic problem the expressions of the observables can be more
655 complicated functions of the lengths (see Refs. [14, 17] as an example) and the corresponding
656 integrals do not give the simple structure of a scalar propagator. On the other hand, for simple
657 problems, whose field theoretical analysis is clear, the propagator structure is recovered by
658 means of the M -layer construction [24].

659 It is also interesting to note that the integrals occurring in field theories are *actually com-*
660 *puted* through the application of formulas like the following:

$$\frac{1}{k^2 + m^2} = \int_0^\infty e^{-l(k^2 + m^2)} dl \quad (\text{B.8})$$

661 see e.g. the appendix to Chap. 5 in [20]. This amounts to go from Eqs. (B.1) and (B.2)
662 back to Eqs. (54) and (55). Thus the M -layer approach directly gives expressions in the above
663 treatable form. Furthermore, the integration variable l , that seems artificial in field theory, has
664 instead the natural meaning of the length of the internal lines of the diagrams in the M -layer
665 approach.

666 C Other diagrams

667 In this appendix we take into account other possible diagrams of order $\mathcal{O}(1/M^2)$ that may
668 contribute to the two-point correlation. As discussed in Ref. [24], the computation of the line
669 without loop should be corrected to $\mathcal{O}(1/M^2)$ by diagram \mathcal{G}'_1 in Fig. 4, with the corresponding

670 weight: $W(\mathcal{G}'_1) = 1/M(1 - 1/M)$. While the contribution of \mathcal{G}'_1 at order $\mathcal{O}(1/M)$ is already
 671 included in Eq. (40), its contribution at order $\mathcal{O}(1/M^2)$ is not included there because \mathcal{G}'_1
 672 diverges with a lower power of μ with respect to \mathcal{G}_2 , which also contributes at order $\mathcal{O}(1/M^2)$.

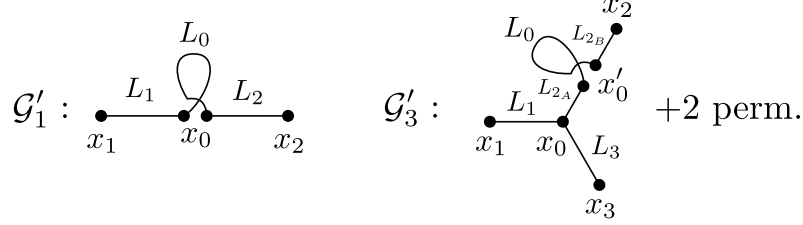


Figure 4: Less divergent diagrams that contribute to the two-point function. Notice that the two couple of vertices in x_0 and x'_0 belong to two different layers while on the projection they are superimposed. The two lines of length L_0 coil themselves in the M -layer lattice, in such a way that the projection on the original lattice looks like a loop.

673 The contribution of \mathcal{G}'_1 at order $\mathcal{O}(1/M^2)$ is

$$-\frac{(2D)^2}{M^2} \frac{(2D)!}{(2D-4)!} \sum_{L_1, L_0, L_2} \sum_{x_0} \mathcal{N}_{L_1}(x_1, x_0) \mathcal{N}_{L_0}(x_0, x_0) \mathcal{N}_{L_2}(x_0, x_2) \mathcal{C}_{2,lc}(\mathcal{G}'_1; L_1, L_0, L_2), \quad (\text{C.1})$$

674 where

$$\mathcal{C}_{2,lc}(\mathcal{G}'_1; L_1, L_0, L_2) = \mathcal{C}_{2,lc}(\mathcal{G}_1; L_1 + L_0 + L_2) = p p^{L_1+L_0+L_2}. \quad (\text{C.2})$$

675 In Fourier space, using Eqs. (51) and (52), it becomes:

$$-(2\pi)^D \delta^D(k_1 + k_2) \frac{(2D)^2}{M^2} \frac{(2D)!}{(2D-4)!} \left(\frac{2D}{2D-1} \right)^3 a_l^{2D} p \frac{1}{\frac{a_l^2}{2D-2} k_1^2 + \mu} \frac{1}{\frac{a_l^2}{2D-2} k_2^2 + \mu} \times \int \frac{d^D k_0}{(2\pi)^D} \int_{\mu/\Lambda^2}^{\infty} d\hat{L}_0 e^{-\left(\frac{a_l^2}{\mu(2D-2)} k_0^2 + 1 \right) \hat{L}_0}, \quad (\text{C.3})$$

676 which can be rewritten by scaling all the momenta, $\hat{k} \equiv k \frac{a_l}{\sqrt{\mu(2D-2)}}$, apart from the ones in
 677 the delta function, as:

$$-(2\pi)^D \delta^D(k_1 + k_2) \frac{(2D)^2}{M^2} \frac{(2D)!}{(2D-4)!} \left(\frac{2D}{2D-1} \right)^3 \mu^{\frac{D}{2}-3} \frac{a_l^D p (2D-2)^{\frac{D}{2}}}{(\hat{k}_1^2 + 1)(\hat{k}_2^2 + 1)} \times \int \frac{d^D \hat{k}_0}{(2\pi)^D} \frac{1}{\hat{k}_0^2 + 1} \propto \frac{\mu^{\frac{D}{2}-3}}{M^2}, \quad (\text{C.4})$$

678 where, as usual, we neglected higher orders in μ setting the lower limit of the length integra-
 679 tion to $\mathbf{0}$. The other contribution to order $\mathcal{O}(1/M^2)$ is from diagram \mathcal{G}_2 , repeating the same
 680 steps we have

$$-(2\pi)^D \delta^D(k_1 + k_2) \frac{(2D)^2}{2M^2} \left(\frac{(2D)!}{(2D-3)!} \right)^2 \left(\frac{2D}{2D-1} \right)^4 \mu^{\frac{D}{2}-4} \frac{a_l^D (2D-2)^{\frac{D}{2}}}{(\hat{k}_1^2 + 1)(\hat{k}_2^2 + 1)} \times \int \frac{d^D \hat{k}}{(2\pi)^D} \frac{1}{\hat{k}^2 + 1} \frac{1}{(\hat{k}_1 - \hat{k})^2 + 1} \propto \frac{\mu^{\frac{D}{2}-4}}{M^2}, \quad (\text{C.5})$$

681 from which it is clear that near the critical point, $\mu \sim \mathbf{0}$, the contribution of \mathcal{G}'_1 can be neglected
 682 with respect to the one of \mathcal{G}_2 . Analogously, diagram \mathcal{G}'_3 , is negligible with respect to \mathcal{G}_4 and
 683 \mathcal{G}_5 . Thus the computations for the three-point correlation function of the main text give the
 684 correct critical behavior.

685 It is also possible to generalize this argument, at least in the case of the percolation prob-
 686 lem. Since for each line of the diagram a factor proportional to $\mu^{-1}(\hat{k}^2 + 1)^{-1}$ appears, we
 687 understand that, at a given order in $\mathcal{O}(1/M)$ the most divergent diagrams, in the limit $\mu \rightarrow \mathbf{0}$
 688 are the ones with the largest number of lines. This argument is not valid generally for any
 689 problem or model. Indeed, the computation of the observables on a given diagram is the only
 690 model-dependent part of the M -layer procedure and in general the result can be a non-trivial
 691 function of the lengths, as we noticed at the end of appendix B.

692 D Four-point correlation function

693 We present, in this appendix, the computation for the most divergent contributions to the four-
 694 point correlation function in the site percolation problem, the same result can be obtained for
 695 the bond percolation with the arguments given in Sec. 5. All the possible topologies, with
 696 only three and four-degree vertices, are shown in Fig. 5.

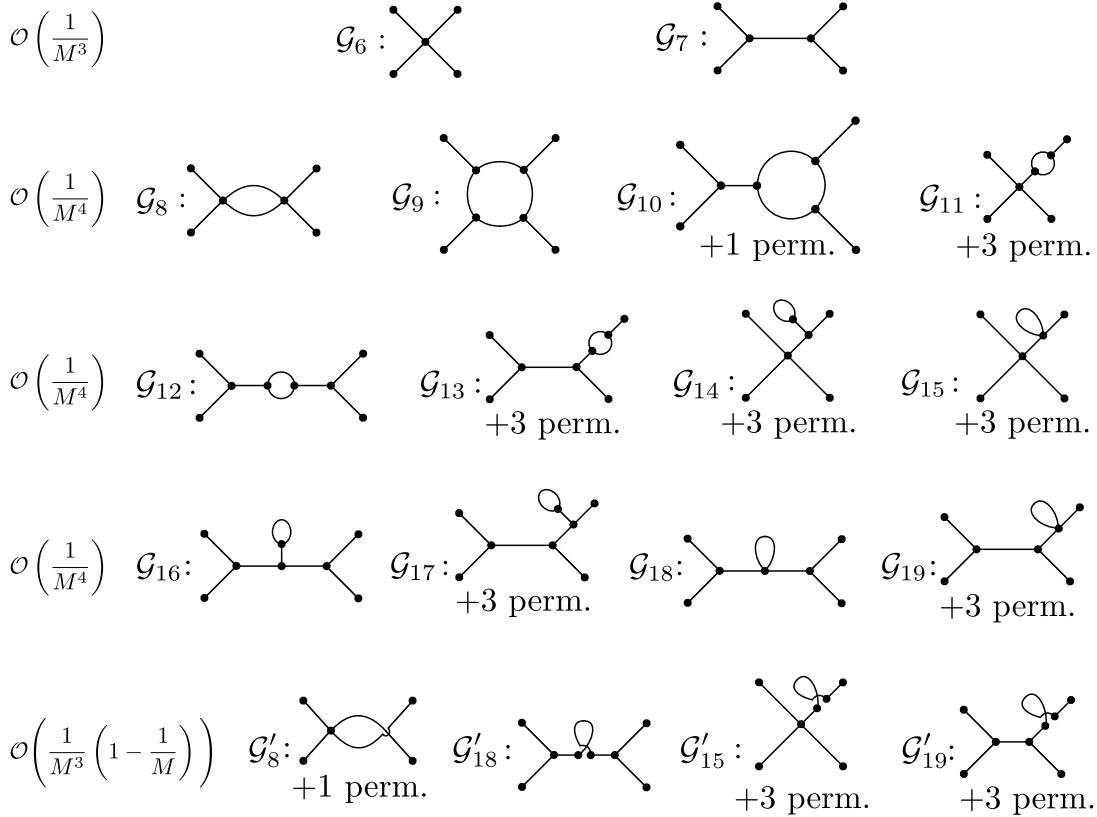


Figure 5: Diagrams contributing to the four-point correlation function up to one loop.

697 Along the lines of the reasoning given for neglecting \mathcal{G}'_1 with respect to \mathcal{G}_2 we identify
 698 the most divergent diagrams to each $\mathcal{O}(1/M)$ order for the four-point correlation function
 699 simply considering the diagrams with the largest number of lines. It turns out that the relevant
 700 diagrams, for the four-point function, are the ones shown in Fig. 6: \mathcal{G}_7 to order $\mathcal{O}(1/M^3)$,
 701 \mathcal{G}_9 , \mathcal{G}_{12} and \mathcal{G}_{13} to order $\mathcal{O}(1/M^4)$. Notice that, in principle, we should have considered also

702 diagrams with vertices of degree larger than four, but they all have, at one loop order, fewer
 703 lines than the ones we included in Fig. 6, thus they are less divergent near the critical point
 704 $\mu \sim 0$.

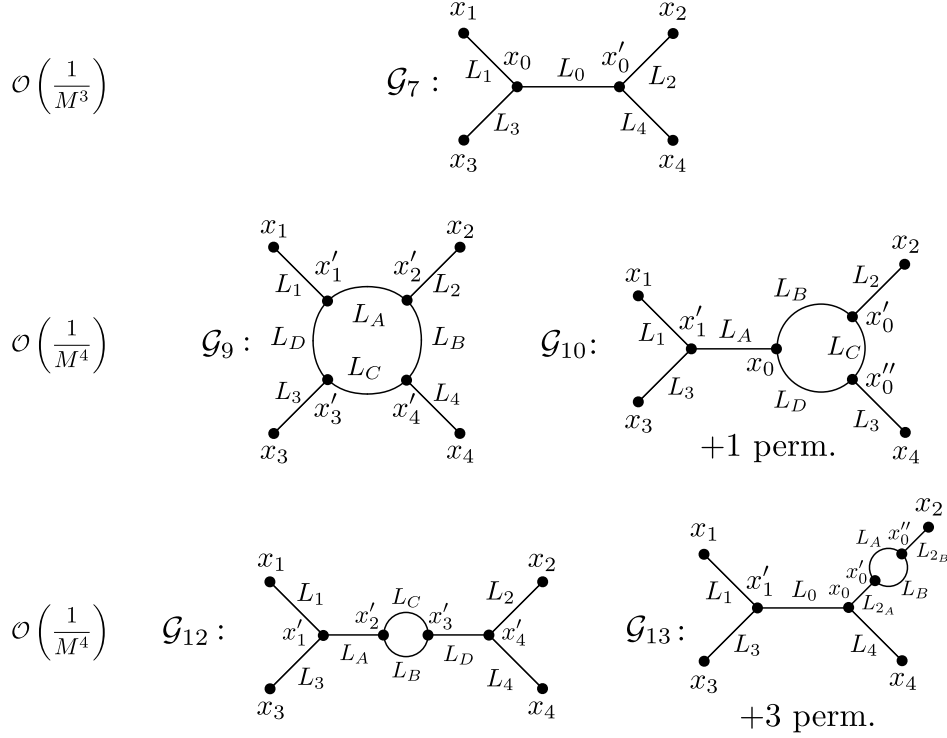


Figure 6: Most divergent diagrams contributing to the four-point correlation functions up to one loop near the critical point.

705 Now we can write the contributions of the identified diagrams:

$$\begin{aligned}
 \overline{C_4(x_1, x_2, x_3, x_4)} = & \\
 & \frac{1}{M^3} \sum_{\vec{L}} \sum_{x_0, x'_0} \mathcal{N}(\mathcal{G}_7; \vec{L}; x_1, x_2, x_3, x_4, x_0, x'_0) C_{4,lc}(\mathcal{G}_7; \vec{L}) + \\
 & + \frac{1}{M^4} \sum_{\vec{L}'} \sum_{\{x'_i, i=1, \dots, 4\}} \mathcal{N}(\mathcal{G}_9; \vec{L}'; x_1, x_2, x_3, x_4, x'_1, x'_2, x'_3, x'_4) C_{4,lc}(\mathcal{G}_9; \vec{L}') + \\
 & + \frac{1}{M^4} \sum_{\vec{L}'} \sum_{x'_1, x_0, x'_0, x''_0} \mathcal{N}(\mathcal{G}_{10}; \vec{L}'; x_1, x_2, x_3, x_4, x'_1, x_0, x'_0, x''_0) C_{4,lc}(\mathcal{G}_{10}; \vec{L}') + \\
 & + \frac{1}{2M^4} \sum_{\vec{L}'} \sum_{\{x'_i, i=1, \dots, 4\}} \mathcal{N}(\mathcal{G}_{12}; \vec{L}'; x_1, x_2, x_3, x_4, x'_1, x'_2, x'_3, x'_4) C_{4,lc}(\mathcal{G}_{12}; \vec{L}') + \\
 & + \frac{1}{2M^4} \sum_{\vec{L}''} \sum_{x'_1, x_0, x'_0, x''_0} \mathcal{N}(\mathcal{G}_{13}; \vec{L}''; x_1, x_2, x_3, x_4, x'_1, x_0, x'_0, x''_0) C_{4,lc}(\mathcal{G}_{13}; \vec{L}'') + \mathcal{O}\left(\frac{1}{M^5}\right),
 \end{aligned} \tag{D.1}$$

706 where the lengths are defined as $\vec{L} = (L_0, L_1, L_2, L_3, L_4)$, $\vec{L}' = (L_1, L_2, L_3, L_4, L_A, L_B, L_C, L_D)$,
 707 $\vec{L}'' = (L_1, L_3, L_4, L_{2A}, L_{2B}, L_A, L_B, L_C, L_D)$, and the NBPs:

$$\mathcal{N}(\mathcal{G}_7; \vec{L}; x_1, x_2, x_3, x_4, x_0, x'_0) = (2D)^4 \left(\frac{(2D)!}{(2D-3)!} \right)^2 \prod_{i=1,3} \mathcal{N}_{L_i}(x_i, x_0) \prod_{i=2,4} \mathcal{N}_{L_i}(x_i, x_0) \mathcal{N}_{L_0}(x_0, x'_0), \quad (\text{D.2})$$

708

$$\mathcal{N}(\mathcal{G}_9; \vec{L}'; x_1, x_2, x_3, x_4, x'_1, x'_2, x'_3, x'_4) = (2D)^4 \left(\frac{(2D)!}{(2D-3)!} \right)^4 \prod_{i=1}^4 \mathcal{N}_{L_i}(x_i, x'_i) \mathcal{N}_{L_A}(x'_1, x'_2) \mathcal{N}_{L_B}(x'_2, x'_4) \mathcal{N}_{L_C}(x'_3, x'_4) \mathcal{N}_{L_D}(x'_3, x'_1), \quad (\text{D.3})$$

709

$$\mathcal{N}(\mathcal{G}_{10}; \vec{L}'; x_1, x_2, x_3, x_4, x'_1, x_0, x'_0, x''_0) = (2D)^4 \left(\frac{(2D)!}{(2D-3)!} \right)^4 \prod_{i=1}^4 \mathcal{N}_{L_i}(x_i, x'_i) \mathcal{N}_{L_A}(x'_1, x_0) \mathcal{N}_{L_B}(x_0, x'_0) \mathcal{N}_{L_C}(x'_0, x''_0) \mathcal{N}_{L_D}(x_0, x''_0), \quad (\text{D.4})$$

710

$$\mathcal{N}(\mathcal{G}_{12}; \vec{L}'; x_1, x_2, x_3, x_4, x'_1, x'_2, x'_3, x'_4) = (2D)^4 \left(\frac{(2D)!}{(2D-3)!} \right)^4 \mathcal{N}_{L_1}(x_1, x'_1) \times \mathcal{N}_{L_2}(x_2, x'_4) \mathcal{N}_{L_3}(x_3, x'_1) \mathcal{N}_{L_4}(x_4, x'_4) \mathcal{N}_{L_A}(x'_1, x'_2) \mathcal{N}_{L_B}(x'_2, x'_3) \mathcal{N}_{L_C}(x'_2, x'_3) \mathcal{N}_{L_D}(x'_4, x'_3), \quad (\text{D.5})$$

711

$$\mathcal{N}(\mathcal{G}_{13}; \vec{L}''; x_1, x_2, x_3, x_4, x'_1, x_0, x'_0, x''_0) = (2D)^4 \left(\frac{(2D)!}{(2D-3)!} \right)^4 \mathcal{N}_{L_1}(x_1, x'_1) \times \mathcal{N}_{L_3}(x_3, x'_1) \mathcal{N}_{L_4}(x_4, x_0) \mathcal{N}_{L_0}(x'_1, x_0) \mathcal{N}_{L_{2B}}(x_2, x''_0) \mathcal{N}_{L_{2A}}(x_0, x'_0) \mathcal{N}_{L_A}(x'_0, x''_0) \mathcal{N}_{L_B}(x'_0, x''_0), \quad (\text{D.6})$$

712 and finally the observables

$$C_{4,lc}(\mathcal{G}_7; \vec{L}) = p p^{L_1+L_2+L_3+L_4+L_0}; \quad (\text{D.7})$$

713

$$C_{4,lc}(\mathcal{G}_9; \vec{L}') = -3p^{L_1+L_2+L_3+L_4+L_A+L_B+L_C+L_D}; \quad (\text{D.8})$$

714

$$C_{4,lc}(\mathcal{G}_{10}; \vec{L}') = -2p^{L_1+L_2+L_3+L_4+L_A+L_B+L_C+L_D}; \quad (\text{D.9})$$

715

$$C_{4,lc}(\mathcal{G}_{12}; \vec{L}') = -p^{L_1+L_2+L_3+L_4+L_A+L_B+L_C+L_D}; \quad (\text{D.10})$$

716

$$C_{4,lc}(\mathcal{G}_{13}; \vec{L}'') = -p^{L_1+L_3+L_4+L_0+L_{2A}+L_{2B}+L_A+L_B}. \quad (\text{D.11})$$

717 Since the identified diagrams, \mathcal{G}_7 , \mathcal{G}_9 , \mathcal{G}_{10} , \mathcal{G}_{12} and \mathcal{G}_{13} , contain only three-degree vertices, we
718 can use the generic equation derived in App. A for this kind of vertices, Eq. (A.7), where

$$f(C_{4,lc}(\mathcal{G}_7; \vec{L}', L_4, L_0)) = 1, \quad (\text{D.12})$$

719

$$f(C_{4,lc}(\mathcal{G}_9; \vec{L})) = -3, \quad (\text{D.13})$$

720

$$f(C_{4,lc}(\mathcal{G}_{10}; \vec{L})) = -2, \quad (\text{D.14})$$

721

$$f(C_{4,lc}(\mathcal{G}_{12}; \vec{L}'')) = -1 = f(C_{4,lc}(\mathcal{G}_{13}; \vec{L}''')) \quad (\text{D.15})$$

722 and $S(\mathcal{G}_7) = S(\mathcal{G}_9) = S(\mathcal{G}_{10}) = 1$, $S(\mathcal{G}_{12}) = 2 = S(\mathcal{G}_{13})$:

$$\begin{aligned}
\overline{\widehat{C}_{4,lc}(\{k_i\}_{i=1,\dots,4})} &= (2\pi)^D \delta^D \left(\sum_{i=1}^4 k_i \right) \frac{\widehat{B}^4 a_l^{3D} \widehat{C}}{\widehat{A} \mu^5} \prod_{i=1}^4 \frac{1}{\widehat{k}_i^2 + 1} \left(\int d\widehat{L}_0 e^{-\widehat{L}_0 - (\widehat{k}_1 + \widehat{k}_3)^2 \widehat{L}_0} + \right. \\
&\quad - 3 \widehat{A} \mu^{\frac{D}{2}-3} \prod_{i=A,B,C,D} \int d\widehat{L}_i e^{-\widehat{L}_i} \int \frac{d^D \widehat{q}}{(2\pi)^D} e^{-\widehat{q}^2 \widehat{L}_A - (\widehat{q} + \widehat{k}_2)^2 \widehat{L}_B - (\widehat{q} + \widehat{k}_2 + \widehat{k}_3)^2 \widehat{L}_C - (\widehat{k}_1 - \widehat{q})^2 \widehat{L}_D} \\
&\quad - 2 \widehat{A} \mu^{\frac{D}{2}-3} \prod_{i=A,B,C,D} \int d\widehat{L}_i e^{-\widehat{L}_i} e^{-(\widehat{k}_1 + \widehat{k}_3)^2 \widehat{L}_A} \int \frac{d^D \widehat{q}}{(2\pi)^D} e^{-\widehat{q}^2 \widehat{L}_B - (\widehat{q} + \widehat{k}_2)^2 \widehat{L}_C - (\widehat{q} + \widehat{k}_2 + \widehat{k}_4)^2 \widehat{L}_D} \\
&\quad - 2 \widehat{A} \mu^{\frac{D}{2}-3} \prod_{i=A,B,C,D} \int d\widehat{L}_i e^{-\widehat{L}_i} e^{-(\widehat{k}_2 + \widehat{k}_4)^2 \widehat{L}_A} \int \frac{d^D \widehat{q}}{(2\pi)^D} e^{-\widehat{q}^2 \widehat{L}_B - (\widehat{q} - \widehat{k}_1)^2 \widehat{L}_C - (\widehat{q} - \widehat{k}_1 - \widehat{k}_3)^2 \widehat{L}_D} \\
&\quad - \frac{\widehat{A} \mu^{\frac{D}{2}-3}}{2} \prod_{i=A,B,C,D} \int d\widehat{L}_i e^{-\widehat{L}_i} e^{-(\widehat{k}_1 + \widehat{k}_3)^2 (\widehat{L}_A + \widehat{L}_D)} \int \frac{d^D \widehat{q}}{(2\pi)^D} e^{-\widehat{q}^2 \widehat{L}_B - (\widehat{q} - \widehat{k}_1 - \widehat{k}_3)^2 \widehat{L}_C} \\
&\quad - \frac{\widehat{A} \mu^{\frac{D}{2}-3}}{2} \sum_{j=1}^4 \prod_{i=0,A,B,j_A,j_B} \int d\widehat{L}_i e^{-\widehat{L}_i} e^{-(\widehat{k}_1 + \widehat{k}_3)^2 \widehat{L}_0 - \widehat{k}_2^2 (\widehat{L}_{j_A} + \widehat{L}_{j_B})} \int \frac{d^D \widehat{q}}{(2\pi)^D} e^{-\widehat{q}^2 \widehat{L}_A - (\widehat{q} + \widehat{k}_j)^2 \widehat{L}_B} \Big) \\
&\quad + \mathcal{O} \left(\frac{1}{M^5} \right). \quad (D.16)
\end{aligned}$$

723 As for the two and three-point correlation functions, we define $\chi_4(\mu)$ as the four-point correlation
724 function at zero external momenta, divided by a_l^{3D} and without the factor $(2\pi)^D \delta^D \left(\sum_{i=1}^4 k_i \right)$:

$$\chi_4(\mu) = \frac{\widehat{B}^4 \widehat{C}}{\widehat{A} \mu^5} \left(1 - \frac{5 \widehat{A} \mu^{\frac{D}{2}-3}}{2 (4\pi)^{\frac{D}{2}}} I_\alpha(\mu) - 4 \frac{\widehat{A} \mu^{\frac{D}{2}-3}}{(4\pi)^{\frac{D}{2}}} I_\gamma(\mu) - 3 \frac{\widehat{A} \mu^{\frac{D}{2}-3}}{(4\pi)^{\frac{D}{2}}} I_\delta(\mu) \right) \quad (D.17)$$

725 where I_α and I_γ are defined in Eqs. (76) and (82) respectively, while

$$I_\delta(\mu) \equiv \int_{\frac{\mu}{\Lambda^2}}^{\infty} d\widehat{L}_A d\widehat{L}_B d\widehat{L}_C d\widehat{L}_D \frac{e^{-\widehat{L}_A - \widehat{L}_B - \widehat{L}_C - \widehat{L}_D}}{(\widehat{L}_A + \widehat{L}_B + \widehat{L}_C + \widehat{L}_D)^{\frac{D}{2}}}, \quad (D.18)$$

726 and consequently

$$\lim_{\mu \rightarrow 0} I_\delta(\mu) = \frac{6-D}{12} \Gamma \left(3 - \frac{D}{2} \right). \quad (D.19)$$

727 Using the relation between μ and m^2 , Eq. (79), we can write χ_4 as a function of m^2

$$\begin{aligned}
\chi_4(\mu(m^2)) &= \frac{\widehat{B}^4 \widehat{C}^{\frac{10}{D}+1}}{\widehat{A} a_l^{10}} m^{-10} \left(1 + \frac{5}{2} \frac{u}{(4\pi)^{\frac{D}{2}}} I_\beta(\mu(m^2)) + \right. \\
&\quad \left. - 4 \frac{u}{(4\pi)^{\frac{D}{2}}} I_\gamma(\mu(m^2)) - 3 \frac{u}{(4\pi)^{\frac{D}{2}}} I_\delta(\mu(m^2)) \right), \quad (D.20)
\end{aligned}$$

728 where u is the bare coupling constant, defined in Eq. (85). Now we can look at the scaling,
729 near the critical point $m^2 \rightarrow 0$, of the four-point function

$$D_4(\lambda) \equiv \left. \frac{\partial \ln \chi_4(\mu(m^2 \simeq 0))}{\partial \ln m^2} \right|_{g \text{ fixed}}, \quad \chi_4(\mu(m^2 \simeq 0)) \sim m^{2D_4(\lambda_c)}. \quad (D.21)$$

730 Using the expression of $\chi_4(m^2)$ we have

$$D_4(\lambda_c) = \frac{1}{42} (D(3D - 55) + 12). \quad (D.22)$$

731 We can now compare with the scaling of the four-point function

$$\chi_q(\mu(m^2 \simeq 0)) \sim m^{2D_q(\lambda_c)}, \quad D_q(\lambda_c) = \frac{q}{4}\eta - \frac{q}{2} + \frac{D}{2}\left(1 - \frac{q}{2}\right), \quad (\text{D.23})$$

732 with $q = 4$, which gives the expected result of Eq. (105)

$$\eta_D = \frac{D-6}{21}. \quad (\text{D.24})$$

733 References

- 734 [1] D. Stauffer and A. Aharony, *Introduction To Percolation Theory: Second Edition*, Taylor &
735 Francis, doi:[10.1201/9781315274386](https://doi.org/10.1201/9781315274386) (1992).
- 736 [2] K. Christensen and N. R. Moloney, *Complexity and Criticality*, PUBLISHED BY IMPE-
737 RIAL COLLEGE PRESS AND DISTRIBUTED BY WORLD SCIENTIFIC PUBLISHING CO.,
738 doi:[10.1142/p365](https://doi.org/10.1142/p365) (2005), <https://www.worldscientific.com/doi/pdf/10.1142/p365>.
- 739 [3] J. W. Essam, *Percolation theory*, Reports on Progress in Physics **43**(7), 833 (1980),
740 doi:[10.1088/0034-4885/43/7/001](https://doi.org/10.1088/0034-4885/43/7/001).
- 741 [4] A. Aharony, *Universal critical amplitude ratios for percolation*, Phys. Rev. B **22**, 400 (1980),
742 doi:[10.1103/PhysRevB.22.400](https://doi.org/10.1103/PhysRevB.22.400).
- 743 [5] P. W. Kasteleyn and C. M. Fortuin, *Phase transitions in lattice systems with random local*
744 *properties* (1969), <https://api.semanticscholar.org/CorpusID:117993636>.
- 745 [6] A. B. Harris, T. C. Lubensky, W. K. Holcomb and C. Dasgupta, *Renormalization-*
746 *group approach to percolation problems*, Phys. Rev. Lett. **35**, 327 (1975),
747 doi:[10.1103/PhysRevLett.35.327](https://doi.org/10.1103/PhysRevLett.35.327).
- 748 [7] D. J. Amit, *Renormalization of the potts model*, Journal of Physics A: Mathematical and
749 General **9**(9), 1441 (1976), doi:[10.1088/0305-4470/9/9/006](https://doi.org/10.1088/0305-4470/9/9/006).
- 750 [8] R. G. Priest and T. C. Lubensky, *Critical properties of two tensor models with application to*
751 *the percolation problem*, Phys. Rev. B **13**, 4159 (1976), doi:[10.1103/PhysRevB.13.4159](https://doi.org/10.1103/PhysRevB.13.4159).
- 752 [9] O. F. de Alcantara Bonfim, J. E. Kirkham and A. J. McKane, *Critical exponents for the*
753 *percolation problem and the yang-lee edge singularity*, Journal of Physics A: Mathematical
754 and General **14**(9), 2391 (1981), doi:[10.1088/0305-4470/14/9/034](https://doi.org/10.1088/0305-4470/14/9/034).
- 755 [10] J. A. Gracey, *Four loop renormalization of ϕ^3 theory in six dimensions*, Phys. Rev. D **92**,
756 025012 (2015), doi:[10.1103/PhysRevD.92.025012](https://doi.org/10.1103/PhysRevD.92.025012).
- 757 [11] M. Borinsky, J. A. Gracey, M. V. Kompaniets and O. Schnetz, *Five-loop renormalization of*
758 *ϕ^3 theory with applications to the lee-yang edge singularity and percolation theory*, Phys.
759 Rev. D **103**, 116024 (2021), doi:[10.1103/PhysRevD.103.116024](https://doi.org/10.1103/PhysRevD.103.116024).
- 760 [12] A. Altieri, M. C. Angelini, C. Lucibello, G. Parisi, F. Ricci-Tersenghi and T. Rizzo, *Loop*
761 *expansion around the bethe approximation through the m -layer construction*, Jour-
762 *nal of Statistical Mechanics: Theory and Experiment* **2017**(11), 113303 (2017),
763 doi:[10.1088/1742-5468/aa8c3c](https://doi.org/10.1088/1742-5468/aa8c3c).

- 764 [13] M. C. Angelini, G. Parisi and F. Ricci-Tersenghi, *One-loop topological expansion for*
765 *spin glasses in the large connectivity limit*, Europhysics Letters **121**(2), 27001 (2018),
766 doi:[10.1209/0295-5075/121/27001](https://doi.org/10.1209/0295-5075/121/27001).
- 767 [14] M. C. Angelini, C. Lucibello, G. Parisi, F. Ricci-Tersenghi and T. Rizzo, *Loop ex-*
768 *ansion around the bethe solution for the random magnetic field ising ferromagnets at*
769 *zero temperature*, Proceedings of the National Academy of Sciences **117**(5), 2268
770 (2020), doi:[10.1073/pnas.1909872117](https://doi.org/10.1073/pnas.1909872117), [https://www.pnas.org/doi/pdf/10.1073/](https://www.pnas.org/doi/pdf/10.1073/pnas.1909872117)
771 [pnas.1909872117](https://www.pnas.org/doi/pdf/10.1073/pnas.1909872117).
- 772 [15] T. Rizzo, *Fate of the hybrid transition of bootstrap percolation in physical dimension*, Phys.
773 Rev. Lett. **122**, 108301 (2019), doi:[10.1103/PhysRevLett.122.108301](https://doi.org/10.1103/PhysRevLett.122.108301).
- 774 [16] T. Rizzo and T. Voigtmann, *Solvable models of supercooled liquids in three dimensions*,
775 Phys. Rev. Lett. **124**, 195501 (2020), doi:[10.1103/PhysRevLett.124.195501](https://doi.org/10.1103/PhysRevLett.124.195501).
- 776 [17] M. C. Angelini, C. Lucibello, G. Parisi, G. Perrupato, F. Ricci-Tersenghi and T. Rizzo, *Unex-*
777 *pected upper critical dimension for spin glass models in a field predicted by the loop expan-*
778 *sion around the bethe solution at zero temperature*, Phys. Rev. Lett. **128**, 075702 (2022),
779 doi:[10.1103/PhysRevLett.128.075702](https://doi.org/10.1103/PhysRevLett.128.075702).
- 780 [18] M. Baroni, G. G. Lorenzana, T. Rizzo and M. Tarzia, *Corrections to the bethe*
781 *lattice solution of anderson localization*, Phys. Rev. B **109**, 174216 (2024),
782 doi:[10.1103/PhysRevB.109.174216](https://doi.org/10.1103/PhysRevB.109.174216).
- 783 [19] H. A. Bethe and W. L. Bragg, *Statistical theory of superlattices*, Proceedings of the
784 Royal Society of London. Series A - Mathematical and Physical Sciences **150**(871), 552
785 (1935), doi:[10.1098/rspa.1935.0122](https://doi.org/10.1098/rspa.1935.0122), [https://royalsocietypublishing.org/doi/pdf/10.](https://royalsocietypublishing.org/doi/pdf/10.1098/rspa.1935.0122)
786 [1098/rspa.1935.0122](https://royalsocietypublishing.org/doi/pdf/10.1098/rspa.1935.0122).
- 787 [20] G. Parisi, *Statistical field theory*, Addison-Wesley (1988).
- 788 [21] J. Zinn-Justin, *Quantum Field Theory and Critical Phenomena*, Oxford University Press,
789 ISBN 9780198509233, doi:[10.1093/acprof:oso/9780198509233.001.0001](https://doi.org/10.1093/acprof:oso/9780198509233.001.0001) (2002).
- 790 [22] A. Coniglio, *Geometrical approach to phase transitions in frustrated and unfrustrated sys-*
791 *tems*, Physica A **281**, 129 (2000), doi:[10.1016/S0378-4371\(00\)00032-7](https://doi.org/10.1016/S0378-4371(00)00032-7).
- 792 [23] M. Mezard, G. Parisi and M. Virasoro, *Spin Glass Theory and Beyond*, WORLD SCIEN-
793 TIFIC, doi:[10.1142/0271](https://doi.org/10.1142/0271) (1986), [https://www.worldscientific.com/doi/pdf/10.1142/](https://www.worldscientific.com/doi/pdf/10.1142/0271)
794 [0271](https://www.worldscientific.com/doi/pdf/10.1142/0271).
- 795 [24] M. C. Angelini, S. Palazzi, G. Parisi and T. Rizzo, *Bethe m-layer construction on the*
796 *ising model*, Journal of Statistical Mechanics: Theory and Experiment **2024**(6), 063301
797 (2024), doi:[10.1088/1742-5468/ad526e](https://doi.org/10.1088/1742-5468/ad526e).
- 798 [25] R. Fitzner and R. van der Hofstad, *Non-backtracking random walk*, Journal of Statistical
799 Physics **150**, 264 (2013), doi:[10.1007/s10955-012-0684-6](https://doi.org/10.1007/s10955-012-0684-6).
- 800 [26] D. J. Amit and V. Martin-Mayor, *Field Theory, the Renormalization Group, and Critical*
801 *Phenomena*, WORLD SCIENTIFIC, 3rd edn., doi:[10.1142/5715](https://doi.org/10.1142/5715) (2005), [https://www.](https://www.worldscientific.com/doi/pdf/10.1142/5715)
802 [worldscientific.com/doi/pdf/10.1142/5715](https://www.worldscientific.com/doi/pdf/10.1142/5715).
- 803 [27] G. Perrupato, M. C. Angelini, G. Parisi, F. Ricci-Tersenghi and T. Rizzo, *Ising spin glass on*
804 *random graphs at zero temperature: Not all spins are glassy in the glassy phase*, Phys. Rev.
805 B **106**, 174202 (2022), doi:[10.1103/PhysRevB.106.174202](https://doi.org/10.1103/PhysRevB.106.174202).